

Ensemble distributional forecasting for insurance loss reserving

Benjamin Avanzi^a, Yanfeng Li^{b,*}, Bernard Wong^b, Alan Xian^c

^aCentre for Actuarial Studies, Department of Economics, University of Melbourne VIC 3010, Australia

^bSchool of Risk and Actuarial Studies, UNSW Business School, UNSW Sydney NSW 2052, Australia

^cDepartment of Actuarial Studies and Business Analytics, Macquarie Business School, Macquarie University NSW 2109, Australia

Abstract

Loss reserving generally focuses on identifying a single model that can generate superior predictive performance. However, different loss reserving models specialise in capturing different aspects of loss data. This is recognised in practice in the sense that results from different models are often considered, and sometimes combined. For instance, actuaries may take a weighted average of the prediction outcomes from various loss reserving models, often based on subjective assessments.

In this paper, we propose a systematic framework to objectively combine (i.e. ensemble) multiple stochastic loss reserving models such that the strengths offered by different models can be utilised effectively. Criteria of choice consider the full distributional properties of the ensemble. A notable innovation of our framework is that it is tailored for the features inherent to reserving data. These include, for instance, accident, development, calendar, and claim maturity effects. Crucially, the relative importance and scarcity of data across accident periods renders the problem distinct from the traditional ensembling techniques in statistical learning.

Our ensemble reserving framework is illustrated with a complex synthetic dataset. In the results, the optimised ensemble outperforms both (i) traditional model selection strategies, and (ii) an equally weighted ensemble. In particular, the improvement occurs not only with central estimates but also relevant quantiles, such as the 75th percentile of reserves (typically of interest to both insurers and regulators).

Keywords: Aggregate Loss reserving, Ensemble learning, Linear Pool, Distributional forecast

JEL Codes: C51, C53, G22

MSC classes: 91G70, 91G60, 62P05, 91B30

1. Introduction

1.1. Background

The prediction of outstanding claims is a crucial process for insurers, in order to establish sufficient reserves for future liabilities, and to meet regulatory requirements. Due to the stochastic nature of future claims payments, insurers not only need to provide an accurate central estimate of the reserve, but they also need to forecast the distribution of reserve accurately. Furthermore, in many countries, provision of the predictive distribution of outstanding claims is required by regulatory authorities. For instance, the Australian Prudential Regulation Authority (APRA) requires general insurers to establish sufficient reserves to cover outstanding claims with at least 75% probability (APRA, 2019). Therefore, insurers need to ensure that their models achieve satisfactory predictive performance beyond the central estimate (expectation) of outstanding claims. This is sometimes referred to as “stochastic loss reserving” (Wüthrich and Merz, 2008).

*Corresponding author.

Email addresses: b.avanzi@unimelb.edu.au (Benjamin Avanzi), yanfeng.li@student.unsw.edu.au (Yanfeng Li), bernard.wong@unsw.edu.au (Bernard Wong), alan.xian@mq.edu.au (Alan Xian)

Early stochastic loss reserving approaches include the distribution-free stochastic Chain-Ladder model proposed by Mack (1993). As computational power increased, Generalised Linear Models (GLMs) became the classical stochastic modelling approach (Taylor and McGuire, 2016). They have been widely applied in both practice and loss reserving literature due to their stochastic nature and high flexibility in modelling various effects on claims payments, such as accident period effects, development period effects, calendar period effects, and effects of claims notification and closure. Common distribution assumption for GLMs include the log-normal distribution (Verrall, 1991), over-dispersed Poisson (ODP) distribution (Renshaw and Verrall, 1998), and gamma distribution (Mack, 1991). Parametric curves to describe claim development patterns, such as the Hoerl curve and the Wright curve (Wright, 1990) can also be incorporated in the GLM context.

In recent years, machine learning models have become popular in loss reserving due to their potential in prediction accuracy as well as the potential for time and cost savings. Notable examples include the smoothing spline (England and Verrall, 2001), Generalised Additive Model for Location, Scale and Shape (GAMLSS) (Spedicato, Clemente and Schewe, 2014), and Neural Networks (Wüthrich, 2018; Kuo, 2019; Al-Mudafer, Avanzi, Taylor and Wong, 2022).

Despite the sophisticated development of loss reserving models, the main focus of current loss reserving literature is to identify a *single* model that can generate the best performance according to some measure of prediction quality. This approach is usually referred to as the “model selection strategy”. However, due to the difference in model structures and assumptions, different loss reserving models are usually specialised at capturing specific claims effects, which are different from one model to the other. However, *multiple* claims effects are typically present in reserving data. Furthermore, these effects are likely to appear inhomogeneously across accident and/or development years (Taylor, 2000; Friedland, 2010). This makes it challenging for a single model to capture all of them. Using a single model to fit claims payments occurred in all accident periods may not be the most effective way to utilise the strengths offered by all the different available models.

Those concerns highlight the potential to develop a model *combination* (as opposed to *selection* strategy).

In practice, ensembles of different deterministic loss reserving models may have been typically constructed based on ad-hoc rules. The weights allocated to component models are commonly selected subjectively based on the model properties (see, e.g., Taylor, 2000; Friedland, 2010). However, due to the subjective nature of this combination strategy, experience based on model properties may not generalise well to new claims data, and the weights allocated to component models are not optimised (Taylor, 2000). Therefore, the information at hand may not be utilised most effectively. The subjective model combination strategy can further cause complications in cases where one wants information on the random distribution of claims. To address this, a more rigorous framework for combining stochastic loss reserving models was developed by Taylor (2000), who proposed to select model weights by minimizing the variance of total estimated outstanding claims. While a great step forward, this approach only considers the first and the second moments of the claims distribution. This may not be sufficient to derive the required quantiles from the distribution of reserves accurately.

The so-called “linear pool” (Gneiting, Raftery, Westveld III and Goldman, 2005), which has been widely applied in combining distributional forecasts outside the field of loss reserving, may offer an alternative model combination approach that could overcome the abovementioned limitations of model selection strategy, and of traditional combination strategies for loss reserving models. The linear pool uses a *proper scoring rule* to determine the weights allocated to component distributional forecasting models. A proper scoring rule assigns a numeric score to a distributional forecasting model when an event materialises. This presents a number of advantages when assessing the quality of distributional forecasts (Gneiting and Raftery, 2007). Literature in the areas of weather forecast (Gneiting et al., 2005; Raftery et al., 2005; Gneiting and Raftery, 2007; Baars and Mass, 2005; Vogel et al., 2018), stocks return forecast, and GDP growth rate forecast (Hall and Mitchell, 2007; McDonald et al., 2011; Opschoor et al., 2017; Hall and Mitchell, 2004) all suggest that linear pool ensembles generate more accurate distributional forecast than any single model in their respective contexts. A common choice for the proper score is the Log Score. In this paper, we start by developing a linear pool approach to loss reserving, and extend the methodology it to best fit the reserving context, as detailed in the following section.

1.2. Statement of contributions

To our knowledge, linear pools have not appeared in the loss reserving literature. Unfortunately, existing linear pool implementations cannot be applied in this context directly for a number of reasons outlined below. This paper aims to fill this gap by developing an adjusted linear pool ensemble forecasting approach that is particularly suitable to the loss reserving context. Although actuaries may combine different loss reserving models in practice, we argued earlier that the model combination is then generally performed subjectively and may not optimise the ensemble’s performance. Compared with the subjective model combination approach, our proposed scheme has two advantages. Firstly, data driven weights reduce the amount of manual adjustment required by the actuary, particularly in cases where a new experience has emerged. Secondly, by using a proper score as the objective function, the distributional forecast accuracy of the ensemble can be optimised. As Shapland (2022) briefly suggests in his monograph, the future development of model combination strategies for loss reserving models should consider the relative predictive power of component models, and the weighted results should “reflect the actuary’s judgements about the entire distribution, not just a central estimate”. Since the proper score can formally assess the quality of distributional forecast, the linear pools satisfy the two conditions proposed by (Shapland, 2022) by using a proper score as the optimisation criterion.

In this paper, we introduce a distributional forecast combination framework that is *tailored* to the loss reserving context. Although the standard ensemble modelling approach has been extensively studied in the literature, it can not be applied directly without modification due to the special data structures and characteristics of the loss reserving data. Specifically, we introduce “**Accident and Development period adjusted Linear Pools (ADLP)**”, which have the following attributes:

- *Triangular shape of aggregate loss reserving data*: To project out-of-sample incremental claims, the **training data must have at least one observation from each accident period and development period** in the upper triangle. Our proposed ensemble ensures that this constraint is satisfied when partitioning the training and validation sets.
- *Time-series characteristics of incremental claims*: Under the standard ensemble approach, the in-sample data is *randomly* split into the training set for training component models and the validation set for estimating combination weights (Breiman, 1996).

However, since the main purpose of loss reserving is to predict future incremental claims, a random split of the data can not adequately validate the extrapolating capability of loss reserving models. In light of the above concern, we **allocate incremental claims from the most recent calendar periods to the validation set** (rather than a randomly selected sample) as they are more relevant to the future incremental claims. This is a common partition strategy used in loss reserving literature (e.g., Taylor and McGuire, 2016). Therefore, the combination weights estimated from the validation set more accurately reflect the component models’ predictive performance on the most recent out-of-sample data.

- *Accident Period effects*: The standard ensemble strategy usually derives its combination weights by using the whole validation set, which implies each component model will receive a single weight for a given data set.

However, it is a very well known fact that the performance of loss reserving models tends to differ by accident periods (Taylor, 2000). Hence, assigning the same weights (for each model) across *all* accident years might not be optimal, and it may be worthwhile allowing those to change over time. To address this, we allow the set of weights to change at arbitrary “split points”. For instance, the set might be calibrated differently for the 10 most recent (immature) accident years.

More specifically, we further **partition the validation set based on accident periods to train potentially different combination weights**, such that the weights can best reflect a models’ performance in the different accident period sets. Our paper shows that the ensemble’s out-of-sample performance can be substantially improved—based on the whole range of evaluation metrics considered here—by adopting the proposed Accident-Period-dependent weighting scheme. Additionally, we also empirically discuss the choice of number and location of accident year split points .

- *Development Period effects*: The accident year split described in the previous item requires some care. One cannot strictly isolate and focus on a given set of accident years (think of a horizontal band) and

use the validation data of that band only as this will lack data from later development years which are required for the projection of full reserves. Hence, we start with the oldest accident year band (or split set), and when moving to the next band, we (i) change the training set according to the accident year effect argument discussed above, but (ii) add the new layer of validation points to the previously used set of validation data when selecting weights for that band.

Note that the data kept from one split to the next is the validation data only, which by virtue of the second item above is always the most recent (last calendar year payments). Hence, this tweak does not contradict the probabilistic forecasting literature’s recommendation of using only the data in the most recent periods (see, e.g. Opschoor, Van Dijk and Van der Wel, 2017) when selecting weights.

- *Data Scarcity*: Data is scarce for aggregate loss reserving, particularly for immature accident periods (i.e., the recent accident periods), where there are only a few observed incremental claims available. A large number of component models relative to the number of observations may cause the prediction or weights estimation less statistically reliable (Aiolfia and Timmermann, 2006). Our proposed ensemble scheme **mitigates this data scarcity issue by incorporating incremental claims from both mature and immature accident periods to train the model weights in immature accident periods.**

The out-of-sample performance of the ADLP is evaluated and compared with single models (model selection strategy), as well as other common model combination methods, such as the equally weighted ensemble, by using synthetic data sets that possess complicated features inspired by real world data.

Overall, we show that our reserving-oriented ensemble modelling framework ADLP yields more accurate distributional forecasts than either (i) a model selection strategy, or (ii) the equally weighted ensemble. The out-performance of the proposed ensembling strategy can be credited to its ability to effectively combine the strengths offered by different loss reserving models and capture the key characteristics of loss reserving data as discussed above. In fact, the mere nature of the challenges described above justify and explain why an ensembling approach is favourable.

1.3. Outline of the paper

In Section 2, we discuss the design and properties of component loss reserving models that will constitute the different building blocks for the model combination approaches discussed in this paper. Section 3 discusses how to best combine those component models, and describes the modelling frameworks of the standard linear pool ensemble and the Accident and Development period adjusted Linear Pools (ADLP) that are tailored to the general insurance loss reserving data. The implementation of our framework is not straightforward, and is detailed in Section 4. Section 5 discusses the evaluation metrics and statistical tests used to assess and compare the performance of different models. The empirical results are illustrated and discussed in Section 6. Section 7 concludes.

2. Choice of component models

Given the extensive literature in loss reserving, which offers a plethora of modelling options, we start by defining criteria for choosing models to include in the ensemble—the “component models”. We then describe the structure of each of the component models we selected, as well as the characteristics of loss data that they aim to capture.

2.1. Notation

We first define the basic notation that will be used in this paper:

- t : the calendar period of incremental claims; $t = i + j - 1$, where i and j denote the accident period and the development period, respectively
- D_{out} : the out-of-sample loss data (i.e. the lower part of an aggregate loss triangle)
- D_{Train} : the loss data used for training component models

- D_{val} : the validation loss data for selecting component models and optimizing the combination weights; D_{Train} and D_{val} constitute the in-sample loss data (i.e. the upper part of an aggregate loss triangle)
- Y_{ij} : the observed incremental claims paid in accident period i and development period j
- \hat{Y}_{ij} : the estimated incremental claims in accident period i and development period j
- R^{True} : the true reserve, defined as $R^{True} = \sum_{i,j \in D_{out}} Y_{ij}$
- \hat{R} : the estimated reserve, defined as $\hat{R} = \sum_{i,j \in D_{out}} \hat{Y}_{ij}$
- N_{ij} : the observed reported claims count occurred in accident period i and development period j
- F_{ij} : the observed number of finalised claims in accident period i and development period j
- $\hat{\mu}_{ij}$: the predicted mean for the distribution of Y_{ij} (or $\ln(Y_{ij})$ for the Log-Normal distribution)
- $\hat{\sigma}_{ij}^2$: the predicted variance for the distribution of Y_{ij} (or $\ln(Y_{ij})$ for the Log-Normal distribution)
- ϕ : the dispersion parameter for the distribution of Y_{ij} ; for distributions coming from Exponential Distribution Family (EDF), $\text{Var}(Y_{ij})$ is a function of ϕ and μ_{ij}
- $\eta_{i,j}$: the linear predictor for incremental claims paid in accident period i and development period j that incorporates information from explanatory variables into the model; $\eta_{i,j} = h^{-1}(\hat{\mu}_{ij})$, where h^{-1} is a link function
- $\hat{f}_m(y_{ij})$: the predicted density by model m evaluated at the observation Y_{ij}

2.2. Criteria for choosing component models

There is a wide range of loss reserving models available in the literature. With an aim to achieve a reasonable balance between diversity and computational cost, we propose the following criteria to select which component models to include in our ensembles:

1. *The component models should be able to fit mechanically without requiring substantial user adjustment in order to avoid the potential subjective bias in model fitting, and to save time spent on manually adjusting each component model.*

This can be of particular concern when there is a large number of component models contained in the ensemble. This criterion is consistent with the current literature on linear pool ensembles, where parametric time-series models with minimum manual adjustments being required are used as component models (Gneiting, Ranjan et al., 2013; Opschoor, Van Dijk and Van der Wel, 2017).

2. *The component models should have different strengths and limitations so as to complement each other in the ensemble.*

This criterion ensures that different patterns present in data can be potentially captured by the diverse range of component models in the ensemble. As Breiman (1996) suggests, having diverse component models could also reduce the potential model correlation, thus improving the reliability and accuracy of the prediction results.

3. *The component models should be easily identifiable and interpretable, and hence are restricted to traditional stochastic loss reserving models and statistical learning models with relatively simple structures.*

Although advanced machine learning models, such as Neural Networks, have demonstrated outstanding potential in forecast accuracy in literature (Kuo, 2019), they might place a substantial challenge on the interpretability of the ensemble and the data size requirement if they are included in the ensemble. Therefore, their implementation into the proposed ensemble has not been pursued in this paper.

In summary, the ensemble should be automatically generated (1), rich (2) and constituted of known and identifiable components (3).

Note, however, that our framework works for any number and type of models in principle, provided the optimisation described in Section 3 can be achieved.

2.2.1. GLM_{CC} : the basic form

The first model included in our ensemble is the GLM with cross-classified structure that has been introduced in modelling outstanding claims since Renshaw and Verrall (1998). The standard cross-classified models can be fitted mechanically, and there is usually no manual adjustment needed for tuning the parameters. Using the notations from Taylor and McGuire (2016), the linear predictor can be specified as

$$\eta_{i,j} = \ln(\alpha_i) + \ln(\beta_j), \quad (2.1)$$

where the accident period effect and development period effect can be captured by the parameters $\ln(\alpha_i)$ and $\ln(\beta_j)$, respectively. Using the log-link function (i.e. $\mu_{i,j} = \exp(\eta_{i,j})$), the predicted incremental claim is modelled as

$$\hat{\mu}_{i,j} = \hat{\alpha}_i \cdot \hat{\beta}_j. \quad (2.2)$$

Therefore, the cross-classified models have the nice interpretation that the predicted incremental claim is the product of the estimated total amount of claims paid in accident period i (i.e. $\hat{\alpha}_i$) and the proportion of that total claims paid in development period j (i.e. $\hat{\beta}_j$). GLM_{CC} is fitted under the Over-Dispersed Poisson (ODP), Gamma, and Log-Normal distribution, which are three common distribution assumptions in loss reserving literature, respectively. The above distribution assumptions are summarised below:

- ODP: $E[Y_{i,j}] = \exp(\eta_{i,j})$ and $\text{Var}(Y_{i,j}) = \phi\mu_{i,j}$;
- Log-Normal: $E[\ln(Y_{i,j})] = \eta_{i,j}$ and $\text{Var}(\ln(Y_{i,j})) = \sigma^2$;
- Gamma: $E[Y_{i,j}] = \mu_{i,j} = \exp(\eta_{i,j})$ and $\text{Var}(Y_{i,j}) = \phi\mu_{i,j}^2$.

Note that GLM_{CC} with the ODP distribution assumption yields the identical central estimate of outstanding claims as to the traditional Chain-Ladder algorithm (Renshaw and Verrall, 1998).

2.2.2. GLM_{Cal} : incorporating calendar period effect

As Taylor and McGuire (2016) commented, calendar period effects can be present due to economic inflation or changes in claims management. Therefore, the second model seeks to capture this effect by introducing the parameter γ in the linear predictor (Taylor and Xu, 2016):

$$\eta_{i,j} = \ln(\beta_j) + t \cdot \ln(\gamma). \quad (2.3)$$

The calendar period effect is assumed to be constant such that the model can be applied mechanically without much users' adjustment based on Criterion 1. GLM_{Cal} is fitted using the same distribution assumptions as GLM_{CC} .

2.2.3. GLM_{HC} : incorporating the Hoerl Curve

The third GLM seeks to capture the shape of development pattern of incremental claims by incorporating a Hoerl curve (Wright, 1990) in the linear predictor, which can be specified as

$$\eta_{i,j} = a_i + b \ln(j) + cj. \quad (2.4)$$

The number of parameters in GLM_{HC} for a 40x40 loss triangle have been significantly reduced from 80 to 42 compared with GLM_{CC} . By adding the Hoerl curve to the ensemble, the potential over-fitting risk of the cross-classified GLM can be mitigated. Similarly, GLM_{HC} is fitted under the ODP, Gamma, and Log-Normal distribution assumptions.

2.2.4. GLM_{PPCI} : incorporating reported claims count information

Incorporating reported (or notified) claims count might lead to better data representation as claim payments could be subject to the impact of claims notification (Taylor and McGuire, 2016), particularly for lines of business with volatile payments but stable average payments per claim (Taylor and Xu, 2016). Following the notations from Taylor and Xu (2016), the linear predictor can be specified as

$$\eta_{i,j} = \ln(\hat{N}_i) + \ln(\beta_j), \quad (2.5)$$

where \hat{N}_i denote the estimated total reported claims count for accident period i . \hat{N}_i can be specified as $\hat{N}_i = \sum_{j=1}^{J-i+1} N_{ij} + \sum_{j=J-i+2}^J \hat{N}_{ij}$, where \hat{N}_{ij} denote the reported claims count that can not be observed and therefore need to be estimated. Following the methodology in Taylor and Xu (2016), \hat{N}_{ij} is estimated from the reported claims count triangle by GLM_{CC} with Over-Dispersed Poisson distribution assumption. GLM_{PPCI} is fitted under the ODP distribution assumption.

2.2.5. GLM_{PPCF} : incorporating finalised claims count information

Incremental claims can also be impacted by the claims closure rate, which can be captured by the PPCF model (Taylor and Xu, 2016). Following the methodology from Taylor and Xu (2016), the payment per finalised claim, defined as Y_{ij}/\hat{F}_{ij} , is modeled by an Over-dispersed Poisson GLM:

$$\hat{\mu}_{ij}^{PPCF} = \exp(\beta_0 + \beta_1 \hat{t}_i(j)), \quad (2.6)$$

where $\hat{t}_i(j)$ is the (estimated) proportion of claims closed up to development period j that are incurred in accident period i , and where \hat{F}_{ij} is estimated by a binomial GLM (Taylor and Xu, 2016). Finally, the estimated incremental claim can be derived as: $\hat{Y}_{ij} = \hat{\mu}_{ij}^{PPCF} \cdot \hat{F}_{ij}$

2.2.6. GLM_{ZALN} and GLM_{ZAGA} : Handling Incremental Claims with Zero Values

In addition to the Over-Dispersed Poisson, Log-Normal, and Gamma distribution assumptions, GLM_{ZALN} and GLM_{ZAGA} are fitted using the Zero-Adjusted Log-Normal (ZALN) distribution and the Zero-Adjusted Gamma (ZAGA) distribution, which are specialised at handling zero incremental claims by assigning a point mass at zero (Resti, Ismail and Jamaan, 2013). Denote the probability mass at zero as ν_j . We assume the point mass to be dependent on development periods, which takes into account the fact that zero incremental claims are more likely to be observed in later development periods when the claims are close to being settled. ν_j can be then modeled by fitting a logistic regression:

$$\hat{\nu}_j = \frac{\exp(\beta_0 + \beta_1 j)}{1 + \exp(\beta_0 + \beta_1 j)}. \quad (2.7)$$

Denote $\hat{\mu}_{ij}^{GA}$ and $\hat{\mu}_{ij}^{LN}$ as the predicted mean for Gamma and Log-Normal distribution, respectively. Finally, the predicted incremental claims under the ZAGA and ZALN distribution can be specified as $\hat{\mu}_{ij}^{ZAGA} = (1 - \hat{\nu}_j)\hat{\mu}_{ij}^{GA}$ and $\hat{\mu}_{ij}^{ZALN} = (1 - \hat{\nu}_j)\hat{\mu}_{ij}^{LN}$, respectively.

2.2.7. Smoothing Spline

Smoothing splines provide a flexible approach to automatically balance data adherence and smoothness. Comparing to fixed parametric curves, smoothing splines have a more flexible shape to incorporate different patterns present in claims development (England and Verrall, 2001). Following the work in England and Verrall (2001), the linear predictor can be specified as

$$\eta_{ij} = s_{\theta_i}(i) + s_{\theta_j}(j), \quad (2.8)$$

where s_{θ_i} are s_{θ_j} are smoothing functions over the accident period i and development period j . The distributional assumption of the smoothing splines implemented in this paper are Normal, Gamma and Log-Normal. The Normal distribution assumption is the original distributional assumption for smoothing spline

in (England and Verrall, 2001), where the latter two distribution assumptions are commonly used in loss reserving literature. For each distributional assumption, the smoothing functions for the accident periods and the development periods are found by maximizing their respective penalised log-likelihoods (Green and Silverman, 1993):

$$l(s_{\theta_i}) = \sum_{i,j} \left(\frac{y_{ij}s_{\theta_i}(i) - \exp(s_{\theta_i}(i))}{\phi} \right) - \theta_i \int (s''_{\theta_i}(t))^2 dt \quad (2.9)$$

$$l(s_{\theta_j}) = \sum_{i,j} \left(\frac{y_{ij}s_{\theta_j}(j) - \exp(s_{\theta_j}(j))}{\phi} \right) - \theta_j \int (s''_{\theta_j}(t))^2 dt; \quad (2.10)$$

where θ_i and θ_j are hyper-parameters that control the degree of smoothness for smoothing spline. The parameters θ_i and θ_j are estimated by minimizing the Generalised Approximate CV Score (GACV) (Gu and Xiang, 2001).

2.2.8. GAMLSS: Generalised Additive Models for Location Scale and Shape

Under the standard GLM setting, the dispersion parameter is assumed to be constant across all accident periods and development periods. However, dispersion levels typically change in practice across development (and sometimes accident) periods (Taylor and McGuire, 2016). By modelling the variance as a function of predictors, GAMLSS, which is firstly proposed by Rigby and Stasinopoulos (2005), might tackle the inconstant dispersion issue automatically (Spedicato, Clemente and Schewe, 2014). Therefore, it is included in our ensembles.

Following the work from Spedicato, Clemente and Schewe (2014), the linear predictor for the distribution mean is in the standard cross-classified form. Although the distribution variance can also be specified in the cross-classified form, to mitigate the potential over-parametrisation risk, a smoothing spline is applied to the development period when modelling the variance term. We also assume the distribution variance to vary only by development periods, which matches the common assumption in loss reserving literature (Taylor and McGuire, 2016). Under the above assumptions, the mean and the variance of the distribution of incremental claims can be modelled as

$$E[Y_{ij}] = g^{-1}(\eta_{1,i,j}) = \exp(\ln(\alpha_i) + \ln(\beta_j)); \quad (2.11)$$

$$\text{Var}[Y_{ij}] = g^{-1}(\eta_{2,i,j}) = \exp(s_{\theta_j}(j)); \quad (2.12)$$

where s_{θ_j} is a smooth function applied here to the development period j only. In this paper, the GAMLSS model is fitted under the distribution assumption of Gamma and Log-Normal, which are common distribution assumptions for loss reserving models.

2.3. Summary of selected component models

Based on the second criterion for choosing component models, each model should have different strengths so that the ensemble can potentially capture various loss reserving data attributes. Table 2.1 summarises the common patterns in claim payments data that actuaries could encounter in modelling outstanding claims, and the corresponding component models that can capture those patterns.

3. Model combination strategies for stochastic ensemble loss reserving

In this section, we first define which criterion we will use for determining the relative strength of one model when compared to another. We then review the two most basic ways of using models within an ensemble: (i) the Best Model in the Validation set (BMV), and (ii) the Equally Weighted ensemble (EW). Both are deficient, in that (i) considers the optimal model, but in doing so discards all other models, and (ii) considers all models, but ignores their relative strength. To improve these and combine the benefits of both approaches, both the Standard Linear Pool (SLP) and Accident and Development period adjusted Linear Pools (ADLP) are next developed and tailored to the reserving context. The section concludes with details of the optimisation routine we used, as well as how predictions were obtained.

Model Class	Model Structures	Fitted Distributions	Effects
GLM Based Model	GLM _{CC}	ODP, Log-Normal, Gamma	accident and development effects
	GLM _{Cal}	ODP, Log-Normal, Gamma	calendar period effects
	GLM _{HC}	ODP, Log-Normal, Gamma	shape of development patterns
	GLM _{PPCI}	ODP	claims notification effects
	GLM _{PPCF}	ODP	claims finalisation effects
	GLM _{ZALN} , GLM _{ZAGA}	ZALN, ZAGA	Occurrence of zero incremental claims
Smoothing Splines	SP	Normal, Log-Normal, Gamma	shape of development patterns
GAMLSS	GAMLSS	Log-Normal, Gamma	varying dispersion

Table 2.1: Summary of component models

3.1. Model combination criterion: the Log Score

We consider “*strictly proper*” scoring rules, which have wide application in probabilistic forecasting literature (Gneiting and Katzfuss, 2014), to measure the accuracy of distributional forecast. Scoring rules assign an numeric score to a distributional forecasting model when an event materialises. Define $S(P, x)$ as the score received by the forecasting model P when the event x is observed, and $S(Q, x)$ as the score assigned to the true model Q . A scoring rule is defined to be “*strictly proper*” if $S(Q, x) \geq S(P, x)$ always holds, and if the equality holds if and only if $P = Q$. The definition of proper scoring rules ensures the true distribution is always the optimal choice, thus encouraging the forecasters to use the true distribution (Gneiting and Raftery, 2007; Gneiting and Katzfuss, 2014). This property is crucial as improper scoring rules can give misguided information about the predictive performance of forecasting models (Gneiting and Raftery, 2007; Gneiting and Katzfuss, 2014).

Furthermore the performance of a distributional forecasting model can be evaluated by its calibration and sharpness. Calibration measures the statistical consistency between the predicted distribution and the observed distribution, while sharpness concerns the concentration of the predicted distribution. A general goal of distributional forecasting is to maximise the sharpness of the predictive distributions, subject to calibration. By using a proper scoring rule, the calibration and sharpness of the predictive distribution can be measured at the same time. For introduction to scoring rules and the advantages of using strictly proper scoring rules, we refer to (Gneiting and Raftery, 2007; Gneiting and Katzfuss, 2014).

In this paper, we use the Log Score, which is a strictly proper scoring rule proposed by Good (1992), to assess our models’ distributional forecast accuracy. It has been commonly applied in evaluating the performance of distributional forecasting models, such as in the fields of financial and economic forecasting (Hall and Mitchell, 2007; McDonald, Thorsrud et al., 2011; Opschoor, Van Dijk and Van der Wel, 2017; Hall and Mitchell, 2004), and weather forecast (Gneiting, Raftery, Westveld III and Goldman, 2005; Raftery, Gneiting, Balabdaoui and Polakowski, 2005; Gneiting and Raftery, 2007; Baars and Mass, 2005; Vogel, Knipptertz, Fink, Schlueter and Gneiting, 2018).

The Log Score has a solid theoretical foundation in the literature. It is closely related to the concept of Log-Likelihood, and the Kullback-Leibler divergence (KLIC) distance between the true density and the predicted density (see Appendix A.1). The Log Score also has a closed-form expression for any distribution with a closed-form density, which makes it computationally inexpensive. A local scoring rule is any scoring rule that depends on a density function only through its value at a materialised event (Parry, Dawid and Lauritzen, 2012). Under certain regularity conditions, it can be shown that every proper local scoring rule is equivalent to the Log Score (Gneiting and Raftery, 2007). For full discussion of the advantages of Log Score, we refer to (Roulston and Smith, 2002; Gneiting and Raftery, 2007).

For a given dataset D , the average Log Score attained by a predictive distribution can be expressed as:

$$\text{LogS} = \frac{1}{|D|} \sum_{i,j \in D} \ln(\hat{f}(y_{i,j})), \quad (3.1)$$

where $\hat{f}(y_{i,j})$ is the predicted density at the observation $y_{i,j}$, and $|D|$ is the number of observations in the dataset D .

Remark 3.1. Here, the Log Score is chosen to calibrate model component weights in the validation sets (the latest diagonals). Strictly proper scoring rules are also used to assess the quality of the distributional forecasting properties of the ensembles developed in this paper, but this time applied in the test sets (in the lower triangle). This is further described in Section 5.

3.2. Best Model in the Validation set (BMV)

Traditionally, a single model, usually the one with the best performance in the validation set, is chosen to generate out-of-sample predictions. In this paper, the Log Score is used as the selection criterion, and the selected model is referred to as the “*best model in validation set*”—abbreviated “**BMV**”. The model selection strategy can be regarded as a special ensemble where a weight of 100% is allocated to a single model (i.e. the **BMV**). Although model selection is based on the relative predictive performance of various models, it is usually hard for a single model to capture all the complex patterns that could be present in loss data (Friedland, 2010). In our alternative ensembles, we aim to incorporate the strengths of different models by combining the prediction results from various models.

3.3. Equally Weighted ensemble (EW)

The simplest *model combination* strategy is to assign equal weights to all component models, which is commonly used as a benchmark strategy in literature (Ranjan and Gneiting, 2010; Hall and Mitchell, 2007; McDonald, Thorsrud et al., 2011). For this so-called “*equally weighted ensemble*”—abbreviated “**EW**”, the combined predictive density can be specified as

$$f_*(y_{ij}) = \sum_{m=1}^M \frac{1}{M} \hat{f}_m(y_{ij}), \quad (3.2)$$

where M is the total number of component models, and $\hat{f}_m(y_{ij})$ is the predicted density from the component model m evaluated at the observation y_{ij} . As the equally weighted ensemble can sometimes outperform more complex model combination schemes (Claeskens, Magnus, Vasnev and Wang, 2016; Smith and Wallis, 2009; Pinar, Stengos and Yazgan, 2012), we also consider it as a benchmark model combination strategy in this paper.

3.4. Standard linear pool ensembles (SLP)

A more sophisticated, while still intuitive approach is to let the combination weights be driven by the data so that the ensemble’s performance can be optimised. A prominent example of such combination strategies in probabilistic forecasting literature is the linear pool approach (Gneiting, Ranjan et al., 2013), which seeks to aggregate individual predictive distributions through a linear combination formula. The combined density function of such “*standard linear pool*”—abbreviated “**SLP**” can be then specified as

$$f^*(y_{ij}) = \sum_{m=1}^M w_m \cdot f_m(y_{ij}) \quad (3.3)$$

at observation y_{ij} , where w_m is the weight allocated to predictive distribution m (Gneiting, Ranjan et al., 2013). Constructing a linear pool ensemble usually involves two stages. In the first stage, the component models are fitted in the training data, and the fitted models will generate predictions for the validation set, which constitute the Level 1 predictions. In the second stage, the optimal combination weights are learned from the Level 1 predictions by maximizing (or minimising) a proper score. Since the weights allocated to component models should reflect their out-of-sample predictive performance, it is important to determine the combination weights by using models’ predictions for the validation set instead of the training set.

Figure 3.1 illustrates the modelling framework for constructing a standard linear pool (SLP) ensemble, with the following steps:

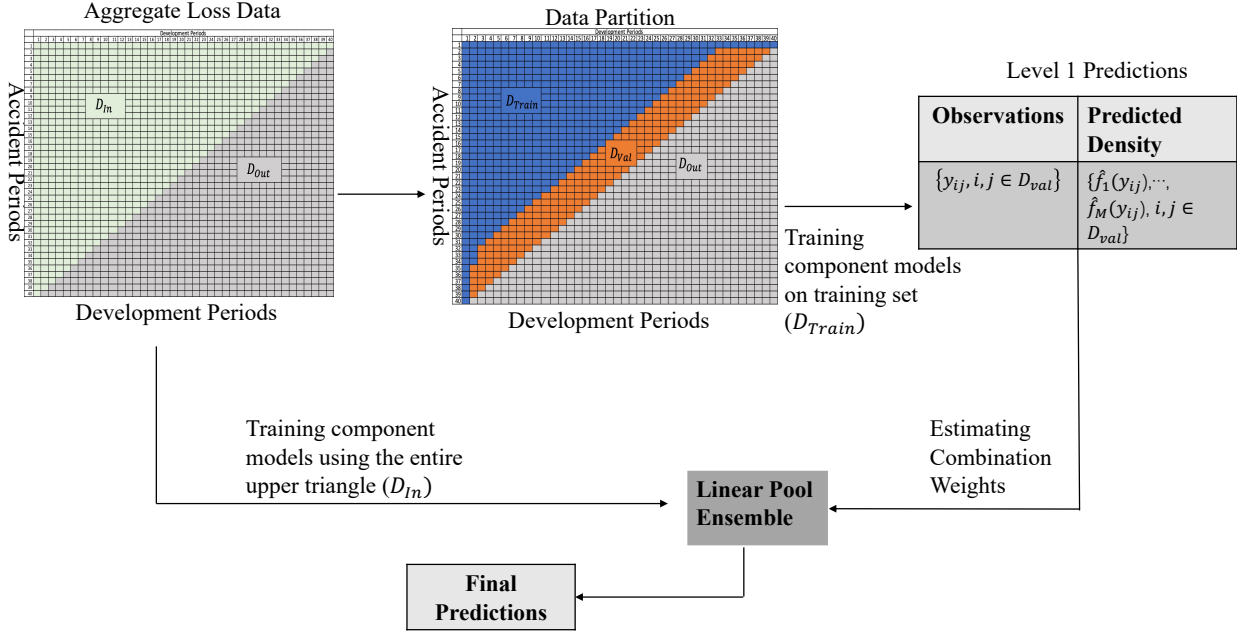


Figure 3.1: Linear Pool Ensemble Framework

1. Partition the in-sample data (i.e. the upper triangle D_{in}) into training set D_{Train} (shaded in blue) and validation set D_{val} (shaded in orange). We allocate the latest calendar periods to the validation set to better validate the projection accuracy of models, which is also common practice in the actuarial literature.
2. Fit the M component models to the training data (i.e. D_{Train}), that is, find the model parameters that maximise the Log Score within D_{Train} (equivalent to Maximum Likelihood estimation).
3. Use the fitted models to generate predicted densities for incremental claims in the validation set, which forms the Level 1 predictions; Denote the Level 1 predictions as $\{\hat{f}_1(y_{ij}), \dots, \hat{f}_M(y_{ij}), i, j \in D^{val}\}$
4. Estimate the optimal combination weights from the Level 1 predictions by maximizing the mean Log-Score achieved by the ensemble, subject to the constraint that combination weights must sum up to one (i.e. $\sum_{m=1}^M w_m = 1$) and each weight should be non-negative (i.e. $w_m \geq 0$). We have then

$$\hat{\mathbf{w}} = \arg \max_{\mathbf{w}} \frac{1}{|D^{val}|} \sum_{y_{ij} \in D^{val}} \ln \left(\sum_{m=1}^M w_m \hat{f}_m(y_{i,j}) \right), \quad (3.4)$$

where $\hat{\mathbf{w}} = [\hat{w}_1, \dots, \hat{w}_M]'$.

The sum-to-unity and non-negativity constraint on model weights are important for two main reasons. Firstly, those constraints ensure the ensemble not to perform worse than the worst component model in out-of-sample data (proof in Appendix B.2). Additionally, the non-negativity constraint can mitigate the potential issue of model correlation by shrinking the weights of some of the highly correlated models towards zero (Coqueret and Guida, 2020; Breiman, 1996).

5. Fit the component models in the entire upper triangle D_{in} , and then use the fitted models to generate predictions for out-of-sample data D_{out} . The predictions are combined using the optimal combination weights determined in step 4.

3.5. Accident and Development period adjusted Linear Pools (ADLP) driven by general insurance characteristics

The estimation of the SLP combination weights specified in (3.4) implies that each model will receive the same weight in all accident periods. However, as previously argued, loss reserving models tend to have different predictive performances in different accident periods, making it potentially ideal for combination weights to vary by accident periods. In industry practice, it is common to divide the aggregate claims triangle by claims maturity and fit different loss reserving models accordingly (Friedland, 2010; Taylor, 2000).

For instance, the PPCF model tends to yield better predictive performance in earlier accident periods (i.e., the more mature accident periods) by taking into account the small number of outstanding claims. In contrast, the PPCI model and the Chain-Ladder tend to have better performance in less mature accident periods as they are insensitive to claims closure (Taylor, 2000). Therefore, in practice, actuaries may want to assign a higher weight to the PPCF model in earlier accident periods and larger weights to the PPCI or Chain-Ladder model in more recent accident periods (Taylor, 2000; Friedland, 2010).

The argument above can be applied to other loss reserving models. To take into account the accident-period-dependent characteristics of loss reserving models, we partition the loss reserving data by claims maturity, with the first subset containing incremental claims from earlier accident periods (i.e., the mature data) and the second subset containing incremental claims from more recent accident periods (i.e., the immature data). The data is thus split an arbitrary number of times K . The weight allocated to component model m for projecting future incremental claims in the k^{th} subset (i.e. D_{test}^k) is then optimised using the k^{th} validation subset (denoted as D_{val}^k):

$$\hat{\mathbf{w}}^k = \arg \max_{\mathbf{w}^k} \frac{1}{|D_{val}^k|} \sum_{y_{i,j} \in D_{val}^k} \ln \left(\sum_{m=1}^M w_m^k \hat{f}_m(y_{i,j}) \right), \quad , k = 1, \dots, K, \quad (3.5)$$

subject to $\sum_{m=1}^M w_m^k = 1, w_m^k \geq 0$. The choice of split points, as well as D_{val}^k require care, as discussed below. We will mainly focus on the case $K = 2$, but this can be easily extended to $K > 2$; see Remark 3.2 below and Appendix C.1, which consider $K = 3$ and briefly discuss how K could be chosen.

Table 3.1: Details of Two-Subsets Data Partition Strategies.

Partition Strategies	Accident Periods in Subset 1	Accident Periods in Subset 2	Proportion in Subset 1
1	2-3	4-40	14%
2	2-5	6-40	23%
3	2-7	8-40	32%
4	2-9	10-40	40%
5	2-11	12-40	47%
6	2-13	14-40	54%
7	2-14	15-40	57%
8	2-15	16-40	60%
9	2-16	17-40	63%
10	2-17	18-40	66%
11	2-18	19-40	69%
12	2-19	20-40	72%
13	2-23	24-40	81%
14	2-26	27-40	87%
15	2-28	29-40	90%
16	2-31	32-40	95%
17	2-33	34-40	97%

Table 3.1 summarises multiple ensembles constructed by using different split points between the two subsets and the corresponding proportion of data points in the upper triangle in the subset 1. We do not test split points beyond accident period 33 due to the scarcity of data beyond this point. Results for all those options will be compared in Section 6, with the objective of choosing the optimal split point.

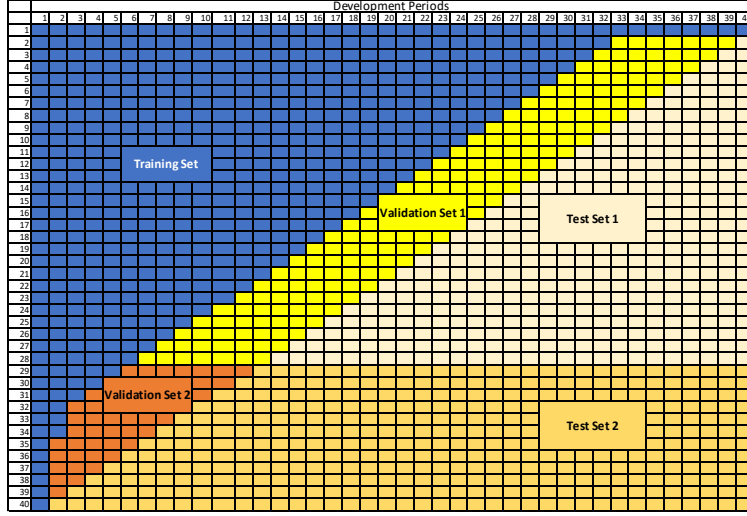


Figure 3.2: Data Partition Diagram: An illustrative example for ensembles that only consider impacts from accident periods

We now turn our attention to the definition of the validation sets to be used in (3.5). This pure “band” approach leads to the definitions depicted in Figure 3.2. Unfortunately this may ignore very important development period effects, because the second validation set (in orange) does not include any of the development periods beyond 12.

More specifically, the training scheme for combination weights specified by (3.5) implies the weights in Subset 2 (i.e. $\hat{\mathbf{w}}^2$) only derive from Subset 2 validation data (i.e. D_{val}^2). However, D_{val}^2 does not capture the late development period effects in out-of-sample data: as shown in Figure 3.2, D_{val}^2 (shaded in orange) contains incremental claims from Development Period 2 to 12. However, D_{test}^2 (shaded in light orange) comprises incremental claims from Development Period 2 to 40. Depending on the lines of business, the impact from late development periods on claims could be quite significant. For example, for long-tailed lines of business, such as the Bodily Injury liability claims, it usually takes a considerably long time for the claims to be fully settled, and large payments can sometimes occur close to the finalisation of claims (Taylor, 2000). In such circumstances, adequately capturing the late development period effects is critically important as missing those effects tends to substantially increase the risk of not having sufficient reserve to cover for those large payments that could occur in the late development periods.

This situation can be exacerbated by the data scarcity issue in D_{val}^2 for ensembles with late split points. For instance, partition strategy 17 only uses claims from Accident Period 34 to 40 in D_{val}^2 , which corresponds to only 20 observations. However, those 20 observations are used to train the 18 model weights. When the data size is small relative to the number of model weights that need to be trained, the estimation of combination weights tend to be less statistically reliable due to the relatively large sampling error (Aiolfia and Timmermann, 2006; Bellman, 1966).

In light of the above concerns, we modify the training scheme such that the mature claims data in D_{val}^1 , which contains valuable information about late development period effects, can be utilised to train the weights in less mature accident periods. Additionally, since both D_{val}^1 and D_{val}^2 are used to train the weights in the second subset, the data scarcity issue in D_{val}^2 can be mitigated. Under the modified training scheme, (3.5) is revised as

$$\hat{\mathbf{w}}^k = \arg \max_{\mathbf{w}^k} \frac{1}{|D_{val}^1 \cup \dots \cup D_{val}^k|} \sum_{y_{i,j} \in D_{val}^1 \cup \dots \cup D_{val}^k} \ln \left(\sum_{m=1}^M w_m^k \hat{f}_m(y_{i,j}) \right), \quad k = 1, \dots, K, \quad (3.6)$$

subject to $\sum_{m=1}^M w_m^k = 1, w_m^k \geq 0$. Since the combination weights estimated using (3.6) take account into impacts and features related to different Accident and Development period combinations, we denote the

resulting ensembles as the **Accident and Development period adjusted Linear Pools (ADLP)**.

An example of data partition strategy under ADLP ensembles with $K = 2$ is given in Figure 3.3 and 3.4, where the new second validation set overlaps the previous first and the second validation set. Since the bottom set uses validation data from all accident periods, its results will hence correspond to the SLP results.

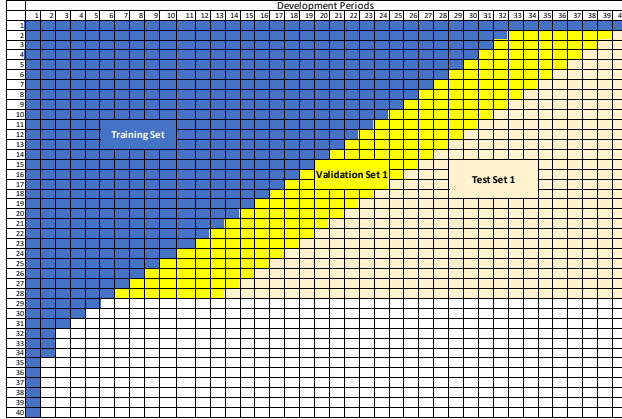


Figure 3.3: ADLP Validation Subset 1

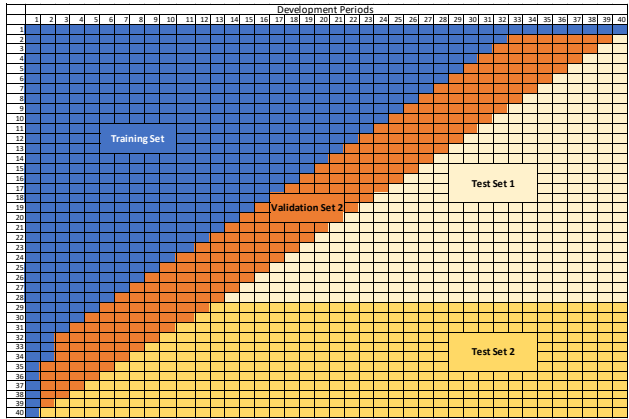


Figure 3.4: ADLP Validation Subset 2

Based on the different partition strategies in Table 3.1, we have seventeen ADLP ensembles in total. We use $ADLP_i$ to denote the ADLP ensemble constructed from the i^{th} partition strategy. The fitting algorithm for ADLP is similar to the algorithm for fitting SLP ensembles described in Section 3.4, except for Step 4, where the combination weights are estimated using (3.6) instead of (3.5).

Remark 3.2. *This paper focuses on the case when $K = 2$ (i.e. partitioning the data into two subsets). However, one can divide the data into more subsets and train the corresponding combination weights by simply using $K > 2$ in (3.6). To illustrate this idea, we provide an example when $K = 3$. For instance, for $ADLP_2$, another split point, say accident period 15, can be introduced after the first split at the accident period 5. We denote the resulting ensemble as $ADLP_2^+$. Similarly, the third subset can be introduced to other ADLP ensembles. Table 3.2 shows some examples of the three-subsets partition strategies based on the current ADLP ensembles.*

Table 3.2: Details of Three-Subsets Data Partition Strategies

Ensembles	Accident Periods in Subset 1	Accident Periods in Subset 2	Accident Periods in Subset 3
$ADLP_2^+$	2-5	6-15	16-40
$ADLP_8^+$	2-15	16-29	30-40
$ADLP_{10}^+$	2-17	18-31	32-40
$ADLP_{13}^+$	2-23	24-33	34-40

The details of the performance analysis of the $ADLP^+$ ensembles listed in Table 3.2 is given in Appendix C.1. Overall, there is no significant difference between the out-of-sample performance of the ADLP ensembles and the corresponding $ADLP^+$ ensembles. At least with the data set used in this study, we do not find enough evidence to support the improvement over the current ADLP ensembles by introducing more subsets for training the combination weights. This phenomenon might be explained by the small difference in the performance of component models after the accident period 20, limiting the ensemble’s potential benefit gained from the diversity among the performance of component models (Breiman, 1996). Therefore, adding additional subsets in the later accident periods seems redundant at least in this example.

Remark 3.3. *Another popular ensemble scheme is the stacked regression approach proposed by Breiman (1996), which uses the Mean Square Error (MSE) as combination criterion. As Yao, Vehtari, Simpson and*

Gelman (2018) suggest, both stacked regression and linear pools correspond to the idea of “stacking”. When MSE is used as optimisation criterion (i.e., the stacked regression approach proposed by Breiman, 1996), the resulting ensemble is a stacking of means. When using the Log Score, the corresponding ensemble is a stacking of predictive distributions.

Although both the stacked regression and linear pools are stacking methods, their objectives are different: the stacked regression seeks to optimise the ensemble’s central forecast accuracy, whereas linear pools strive to optimise the calibration and sharpness of distributional forecast. When combining distributional forecasts, Yao, Vehtari, Simpson and Gelman (2018) suggest using linear pools rather than the stacked regression. This is because MSE is not a strictly proper scoring rule, which might cause identification issues (Yao, Vehtari, Simpson and Gelman, 2018). Therefore, we focus on the application of linear pools in this paper.

4. Implementation of the SLP and ADLP

This section is dedicated to the implementation of the SLP and ADLP framework. It provides theoretical details for such implementation, and it complements the codes available at <https://github.com/agi-lab/reserving-ensemble>.

4.1. Minorization-Maximization strategy for Log Score optimisation

To solve the optimisation problem specified in (3.5) and (3.6), we implement the Minorization-Maximization strategy proposed by Conflitti, De Mol and Giannone (2015) which is a popular and convenient strategy for maximizing the Log Score. Instead of directly maximizing the Log Score, a surrogate objective function is maximised. Define

$$\phi_\lambda(w_m^k, a) = \frac{1}{|D_{val}^{k*}|} \sum_{y_{ij} \in D_{val}^{k*}} \sum_{m=1}^M \frac{\hat{f}_m(y_{i,j}) a_m}{\sum_{l=1}^M \hat{f}_l(y_{i,j}) a_l} \ln \left(\frac{w_m^k}{a_m} \sum_{l=1}^M \hat{f}_l(y_{i,j}) a_l \right) - \lambda \left(\sum_{m=1}^M w_m^k \right), \quad (4.1)$$

where a_m is an arbitrary weight, λ is a Lagrange Multiplier, and where $D_{val}^{k*} = D_{val}^1 \cup \dots \cup D_{val}^k$. Note that for the SLP, we have $w_m^1 = \dots = w_m^k \equiv w_m$. The weights are then updated iteratively by maximizing (4.1):

$$(w_m^k)_{i+1} = \arg \max_w \phi_\lambda(w_m^k, (w_m^k)_i). \quad (4.2)$$

By setting

$$\frac{\partial \phi_\lambda(w_m^k, (w_m^k)_i)}{\partial w_m^k} = 0,$$

we have

$$w_m^k = \frac{1}{\lambda} \frac{1}{|D_{val}^{k*}|} \sum_{y_{ij} \in D_{val}^{k*}} \frac{\hat{f}_m(y_{i,j})(w_m^k)_i}{\sum_{l=1}^M \hat{f}_l(y_{i,j})(w_l^k)_i}.$$

Now, using the constraint $\sum_{m=1}^M w_m^k = 1$ yields

$$\sum_{m=1}^M w_m^k = \frac{1}{\lambda} \frac{1}{|D_{val}^{k*}|} \sum_{y_{ij} \in D_{val}^{k*}} \frac{\sum_{m=1}^M \hat{f}_m(y_{i,j})(w_m^k)_i}{\sum_{l=1}^M \hat{f}_l(y_{i,j})(w_l^k)_i} = \frac{1}{\lambda} \frac{1}{|D_{val}^{k*}|} \sum_{y_{ij} \in D_{val}^{k*}} 1 = \frac{1}{\lambda} \cdot \frac{|D_{val}^{k*}|}{|D_{val}^{k*}|} = \frac{1}{\lambda} = 1.$$

Therefore, $\lambda = 1$, and the updated weights in each iteration become:

$$(w_m^k)_{i+1} = (w_m^k)_i \sum_{y_{ij} \in D_{val}^{k*}} \frac{\hat{f}_m(y_{i,j})}{\sum_{l=1}^M \hat{f}_l(y_{i,j})(w_l^k)_i}, \quad (4.3)$$

where the weights will be initialised as $(w_m^k)_0 = 1/M$ such that the constraints $\sum_{m=1}^M w_m^k = 1$ and $w_m^k \geq 0$ can be automatically satisfied in each iteration. The iterations of weights are expected to converge due to

the monotonically increasing property of the surrogate function (Conflitti, De Mol and Giannone, 2015). To promote computational efficiency, the algorithm is usually terminated when the difference between the resulting Log Scores from the two successive iterates is less than a tolerable error ϵ (Conflitti, De Mol and Giannone, 2015). We set $\epsilon = 10^{-6}$, which is a common tolerable error used in the literature. An outline for the Minorization-Maximization Strategy is given in Algorithm 1.

Algorithm 1 Minorization-Maximisation algorithm for Log Score maximisation

- 1: Initialise $(w_1^k)_0 = (w_2^k)_0 = \dots, (w_M^k)_0 = \frac{1}{M}$
 - 2: $i \leftarrow 0$
 - 3: $\overline{\text{LogS}}_i^k \leftarrow \frac{1}{|D_{val}^{k*}|} \sum_{y_{ij} \in D_{val}^{k*}} \ln(\sum_{m=1}^M (w_m^k)_0 \cdot \hat{f}_m(y_{i,j}))$
 - 4: **while** $\overline{\text{LogS}}_{i+1}^k - \overline{\text{LogS}}_i^k > 10^{-6}$ **do**
 - 5: Update the combination weights: $(w_m^k)_{i+1} = (w_m^k)_i \sum_{y_{ij} \in D_{val}^{k*}} \frac{\hat{f}_m(y_{i,j})}{\sum_{l=1}^M \hat{f}_l(y_{i,j})(w_l^k)_i}$
 - 6: $i = i + 1$
 - 7: **end while**
-

Note that this process can be used to optimise 3.4, as this is a special case of the ADLP with $K = 1$.

4.2. Prediction from Ensemble

Based on (3.3), the central estimate of incremental claims by the ensemble can be calculated using Lemma 4.1, with proof in Appendix B.3:

Lemma 4.1. $\mu_{ij}^* = \sum_{m=1}^M w_m \cdot \mu_{ij}^m$.

To avoid abuse of notation, w_m in this section can be either the weight under SLP or the weight under ADLP. For ADLP ensembles, w_m is set to w_m^k in the calculation below if $y_{ij} \in D^k$.

To provide a central estimation for reserve, we simply aggregate all the predicted mean in the out-of-sample data: $\hat{R}^* = \sum_{i,j \in D_{out}} \mu_{ij}^*$. Since insurers and regulators are also interested in the estimation of 75th reserve quantile, simulation is required. Since the predicted distribution by the linear pool ensemble can be identified as a mixture distribution by (3.3), the weight allocated to a component model can be interpreted as the probability associated with that component distribution. For instance, if a random variable is drawn from the mixture distribution, then there is a probability of w_m that the random variable is drawn from the component distribution m . Therefore, simulation for the linear pool ensemble usually involves two stages. Firstly, a random variable is simulated from Uniform(0, 1) distribution, denoted as U . If $U \in [\sum_{m=1}^{l-1} w_m, \sum_{m=1}^l w_m)$, then a random variable is simulated from the l^{th} component distribution by using Lemma 4.2, with proof in Appendix B.4:

Lemma 4.2. *The probability that a randomly drawn variable from the Uniform(0, 1) distribution falls in the range $(\sum_{m=1}^{l-1} w_m, \sum_{m=1}^l w_m]$ is w_l .*

The algorithm outline for simulating the 75th reserve quantile for linear pool ensemble is summarised in Algorithm 2.

5. Comparison of the predictive performance of the ensembles

5.1. Measuring distributional forecast accuracy: Log Score

To assess and compare the out-of-sample distributional forecast performance of different models, the Log Score is averaged across all the cells in the lower triangle :

$$\text{LogS}^{out} = \frac{1}{|D^{out}|} \sum_{i,j \in D^{out}} \ln(\hat{f}(y_{i,j})). \quad (5.1)$$

Algorithm 2 Algorithm for simulating reserve quantile from linear pools ensembles

- 1: Simulate N random variables from $\text{Uniform}(0, 1)$; Denote $\tilde{U} = (\tilde{U}_{(1)}, \dots, \tilde{U}_{(N)})$ as the vector of N simulated Uniformly distributed random variables
 - 2: Denote $\tilde{Y}_{ij}^* = (\tilde{Y}_{ij,(1)}^*, \dots, \tilde{Y}_{ij,(N)}^*)$ as the vector of N simulated variables for cell (i, j) from the ensemble
 - 3: **for** $n = 1, \dots, N$ **do**
 - 4: **if** $\tilde{U}_{(n)} \in (\sum_{m=1}^{l-1} w_m, \sum_{m=1}^l w_m]$ **then**
 - 5: simulate a random variable from the l^{th} component distribution, denoted as $\tilde{Y}_{ij}^{(l)}$
 - 6: Set $\tilde{Y}_{ij,(n)}^* = \tilde{Y}_{ij}^{(l)}$
 - 7: **end if**
 - 8: **end for**
 - 9: Repeat the above two steps for each cell (i, j)
 - 10: Calculate the simulated reserve based on the simulated random variables for each cell (i, j) : $\tilde{R}^* = (\tilde{R}_{(1)}^*, \tilde{R}_{(2)}^*, \dots, \tilde{R}_{(N)}^*) = (\sum_{i,j \in D^{\text{out}}} \tilde{Y}_{ij,(1)}^*, \sum_{i,j \in D^{\text{out}}} \tilde{Y}_{ij,(2)}^*, \dots, \sum_{i,j \in D^{\text{out}}} \tilde{Y}_{ij,(N)}^*)$
 - 11: Calculate the empirical 75th quantile of the N simulated reserves for the ensemble: R_{75}^*
-

Since loss reserving models tend to perform differently in different accident periods, we also summarise the Log Score by accident periods:

$$\text{LogS}_{\text{AP}_i}^{\text{out}} = \frac{1}{|D_{\text{AP}_i}^{\text{out}}|} \sum_{j \in D_{\text{AP}_i}^{\text{out}}} \ln(\hat{f}(y_{i,j})), \quad (5.2)$$

where $D_{\text{AP}_i}^{\text{out}}$ denotes the set of out-of-sample incremental claims in accident period i .

5.2. Measuring distributional forecast accuracy: CRPS

Besides Log Score, another popular proper score in evaluating distributional forecasting performance and model combination is the Continuously Ranked Probability Score (CRPS) (Gneiting and Ranjan, 2011; Opschoor, Van Dijk and Van der Wel, 2017). Formally, a predictive distribution with cumulative distribution function F_m will attain a CRPS of

$$\text{CRPS}(F_m, y_k) = \int_{-\infty}^{\infty} (F_m(z) - \mathbb{I}_{z \geq y_k})^2 dz \quad (5.3)$$

at observation y_k (Gneiting and Ranjan, 2011). This will need to be discretised; details are provided in Appendix A.2.

The CRPS can be interpreted as a measurement of the difference between the predicted and observed cumulative distributions (Hersbach, 2000); see Appendix A.2. In this paper, the proposed methods are also evaluated using the CRPS as an independent score.

5.3. Statistical tests

To determine whether the difference between the performance of two competing forecasting models is statistically significant, statistical tests are necessary. We consider the Diebold-Mariano test in this paper due to its high flexibility and wide application in probabilistic forecasting literature (Diebold and Mariano, 1995; Gneiting and Katzfuss, 2014). Diebold-Mariano test is one of the few tests that does not require loss functions to be quadratic and the forecast errors to be normally distributed, which is what we need in our framework.

Consider the null hypothesis stating that model G has equal performance as model F . The Diebold-Mariano test statistic can then be specified as (Diebold and Mariano, 1995)

$$t_n = \sqrt{n} \frac{\bar{S}_n^F - \bar{S}_n^G}{\hat{\sigma}_n}. \quad (5.4)$$

where \bar{S}_n^F and \bar{S}_n^G are the average scores (here, Log Score) received by models F and G in out-of-sample data, and where $\hat{\sigma}_n$ is the estimated standard deviation of the score differential. That is,

$$\hat{\sigma}_n = \sqrt{\frac{1}{|D^{out}|} \sum_{i,j \in D^{out}} (\ln(\hat{f}_F(y_{i,j})) - \ln(\hat{f}_G(y_{i,j})))^2}. \quad (5.5)$$

Assuming the test statistic to asymptotically follow a standard Normal distribution, the null hypothesis will be rejected at the significance level of α if the test statistic is greater than the $(1 - \alpha)$ quantile of the standard Normal distribution. We also consider the Adjusted Diebold-Mariano test proposed by Diebold and Mariano (2002) in this paper, which is suggested to work well when the serial correlation and contemporaneous correlation are present. Details can be found in Appendix A.3.

5.4. Measuring performance on the aggregate reserve level

On the aggregate level, the central estimate for reserve by model m is assessed by the relative reserve bias:

$$R^{bias} = \frac{\hat{R}^m - R^{True}}{R^{True}}. \quad (5.6)$$

Since insurers and regulators are also interested on the estimation of the 75th quantile of reserve, a model is also assessed by its relative reserve bias at the 75th quantile:

$$R_{75}^{bias} = \frac{\hat{R}_{75}^m - R_{75}^{True}}{R_{75}^{True}}, \quad (5.7)$$

where R_{75}^{True} is the 75th quantile of the true outstanding claims, and \hat{R}_{75}^m is the estimated 75th quantile by model m . The calculation details for \hat{R}_{75}^m can be found in Appendix B.1.

Remark 5.1. *Of course, R^{True} and R_{75}^{True} are not observable in practice. Thanks to our use of simulated data (see Section 6.1) though, we are able to calculate those from the full simulations and here have been calculated using simulated data in the bottom triangles. The reserve R^{True} is simply the average of the sum of payments in the bottom triangle, and R_{75}^{True} can be taken to be the empirical 75th of the true reserves.*

6. Results and discussion

After presenting the ensemble modelling framework, this section provides numerical examples to illustrate the out-of-sample performance of the proposed linear pool ensembles SLP and ADLP, as well as the BMV and EW. Following the introduction of the synthetic loss reserving data in Section 6.1, Section 6.2.1 and Section 6.2.2 analyse the distributional forecast performance of the SLP and the ADLP ensembles on incremental claims level, respectively. Section 6.2.3 analyses the difference in models' performance using statistical test results. The performance of the proposed ensembles is also analysed at the aggregate reserve level in Section 6.4. Finally, we share some insights on the properties of component models by analysing the optimal combination weights yielded by our framework.

6.1. Example data

Our models are tested using the SynthETIC simulator (Avanzi, Taylor, Wang and Wong, 2021a,b), from which triangles for aggregate paid loss amounts, reported claim counts, and finalised claim counts are generated and aggregated into 40x40 triangles. To better understand the models' predictive performance and test the consistency of the performance, 100 loss data sets are simulated, and models are fit to each of the 100 loss data sets.

Simulated data is preferred in this study as it allows the models' performance to be assessed over the distribution of outstanding claims, and the quality of distribution forecast is the main focus of this paper. This paper uses the default version of SynthETIC, with the following key characteristics (Avanzi, Taylor, Wang and Wong, 2021a,b):

- Claim payments are long-tailed: In general, the longer the settlement time, the more challenging it is to provide an accurate estimate of the reserve due to more uncertainties involved; (Jamal, Canto, Fernwood, Giancaterino, Hiabu, Invernizzi, Korzhynska, Martin and Shen, 2018)
- High volatility of incremental claims;
- Payment size depends on claim closure: The future paid loss amount generally varies in line with the finalisation claims count (i.e. the number of claims being settled), particularly in earlier accident periods.

The key assumptions above are inspired by features observed in real data and aim to simulate the complicated issues that actuaries can encounter in practice when modelling outstanding claims (Avanzi, Taylor, Wang and Wong, 2021a). With such complex data patterns, it is challenging for a single model to capture all aspects of the data. Therefore, relying on a single model might increase the risk of missing important patterns present in the data.

6.2. Predictive performance at the incremental claims level

In terms of distributional forecast accuracy, the linear pool ensembles SLP and ADLP outperform both the EW ensemble and the BMV **at the incremental claims level**, measured by the average Log Score over 100 simulations. Furthermore when appropriately partitioning the validation data into two subsets, the performance of the ADLP is better than that of the SLP.

6.2.1. SLP: the Standard Linear Pool ensemble

The distribution of the Log Score received by SLP, BMV, EW (i.e., the equally weighted ensemble) is illustrated in Figure 6.1. Even without any partition of the validation set for training combination weights, the linear pool ensemble achieves a higher average Log Score than its competing strategies (which means it is preferred), with similar variability in performance.

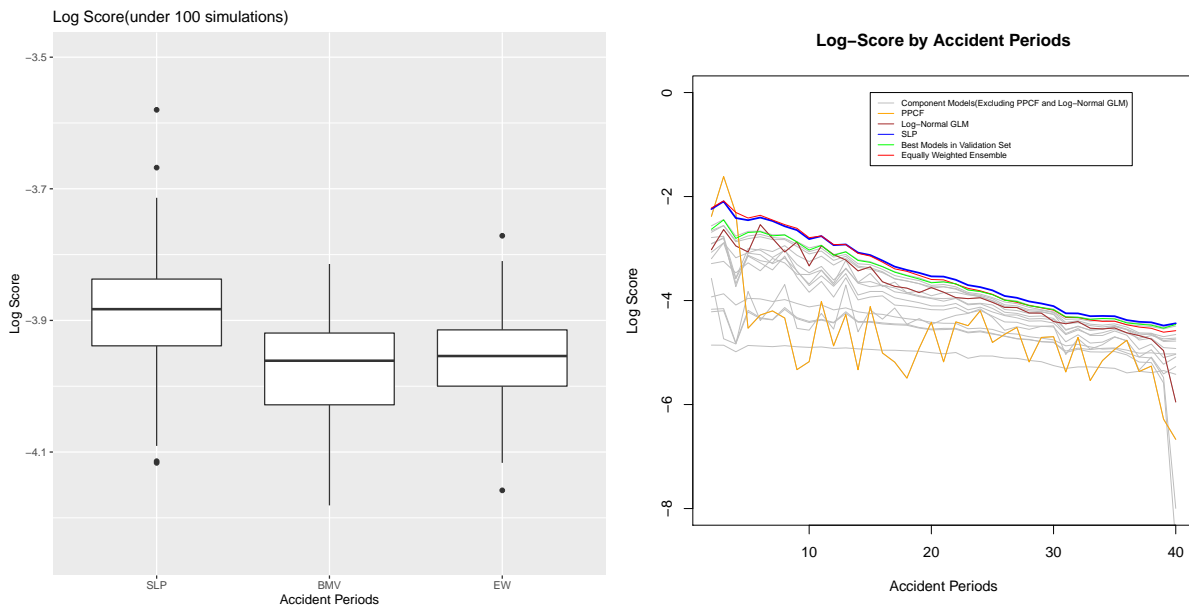


Figure 6.1: Distribution of Log Score over 100 simulations Figure 6.2: Mean Log Score by accident periods (higher (higher is better): comparison among SLP, BMV and EW is better)

The performance of different methods in each accident period is illustrated in Figure 6.2, which shows the Log Score by accident periods being calculated using (5.2), averaging over 100 simulations. The SLP

strictly outperforms the BMV in all accident periods. Although the BMV, which is the smoothing spline with Log-Normal distributional assumption (i.e., SP_{LN}) in this example, has the highest **average** Log Score among the component models, it does not yield the best performance in every accident period. For instance, the BMV under-performs the PPCF model in accident periods 2 and 3, and it is beaten by Log-Normal GLM in accident period 5. Therefore, the common model selection strategy, which relies on the BMV to generate predictions for all accident periods, might not be the optimal solution.

Additionally, the SLP strictly outperforms the equally weighted ensemble after accident period 20. The under-performance of the equally weighted ensemble might be explained by the relatively poor performance of several models in late accident periods, which drag down the Log Score attained by the equally weighted ensemble. Therefore, despite the simplicity of the equally weighted ensemble, blindly assigning equal weight to all component models tends to ignore the difference in the component models' strengths and might increase the risk of letting a few inferior models distort the ensemble's performance.

However, there is no substantial improvement over the equally weighted ensemble brought by SLP at the earlier half of the accident periods. The unsatisfactory predictive performance of SLP at earlier accident periods (i.e., mature accident periods) might be explained by the fact that a component model receives the same weight across all accident periods under the SLP, which is what motivated the development of the ADLP in Section 3.5. More specifically, and in this example, although the PPCF and the Log-Normal GLM have relatively low overall Log Score due to their poor performance in immature accident periods, they have the best predictive performance among the component models at mature accident periods. However, since the weight allocated to each model reflects its overall predictive performance in all accident periods, the PPCF and the Log-Normal GLM are assigned small weights as shown in Figure C in Appendix C.2, regardless of their outstanding predictive performance in earlier accident periods. The ADLP offers a solution to this problem, as illustrated in the following section.

6.2.2. $ADLP_1$ to $ADLP_{17}$: Linear Pool ensembles with different data partition strategies

Figure 6.3 plots the **out-of-sample** Log Score attained by ADLP ensembles with the different split points specified in Table 3.1, averaging over 100 simulations. The blue point represents the mean Log Score attained by SLP, which is a special case of ADLP ensemble with split point at accident period 0 (i.e., there is no subset). All the ADLP ensembles outperform SLP based on Log Score, supporting the advantages of data partitioning as discussed in previous sections.

As per Figure 6.3, the mean Log Score forms an inverse U shape, with the peak when splitting at accident period 15. The shape of the mean Log Score can be explained by the following reasons. If the split point is too early (e.g., split point at accident period 3), there is little improvement brought by ADLP over SLP due to the small number of data points in the first subset. This idea can also be illustrated in Figure 6.4, which dissects the ensembles' performance into accident periods. Although $ADLP_1$, represented by the orange line in Figure 6.4, has the best performance in the second and third accident period, its Log Score falls to the SLP's level afterward. Therefore, the overall difference between $ADLP_1$ and SLP is relatively tiny. As more accident periods are incorporated into the first subset, there is a greater overall difference between ADLP ensembles and SLP, which explains the increasing trend of mean Log Score before accident period 15.

However, for late split points (e.g., the split point at accident period 33), the performance of ADLP ensembles also tends to SLP as shown in Figure 6.4. This is because the first subset of those ADLP ensembles with late split points covers most of the accident periods, and the SLP can be interpreted as a special case of ADLP ensembles with one set that includes all accident periods. Additionally, late split points might make it hard for the ensemble to focus on and thus take advantage of the high-performing models in earlier accident periods.

Based on the above reasoning, an ideal partition strategy should balance the ensemble's performance in both earlier and later accident periods. In this study, the optimal split point is attained at accident period 15, which partitions 60% of the number of incremental claims to the first subset. As per Figure 6.4, $ADLP_8$, which has a split point on accident period 15, substantially outperforms its competitors in the first fifteen accident periods by effectively capturing the high Log Score attained by a few outstanding models.

However, we want to acknowledge that this example is for illustration purposes. The recommendation made above may be more relevant to the loss data sets that share similar characteristics with the synthetic

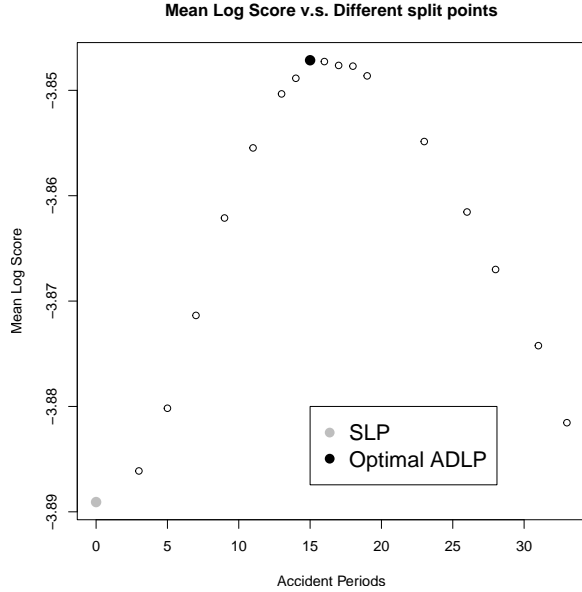


Figure 6.3: Mean Log Score Plot: comparison among different partition strategies (higher is better)

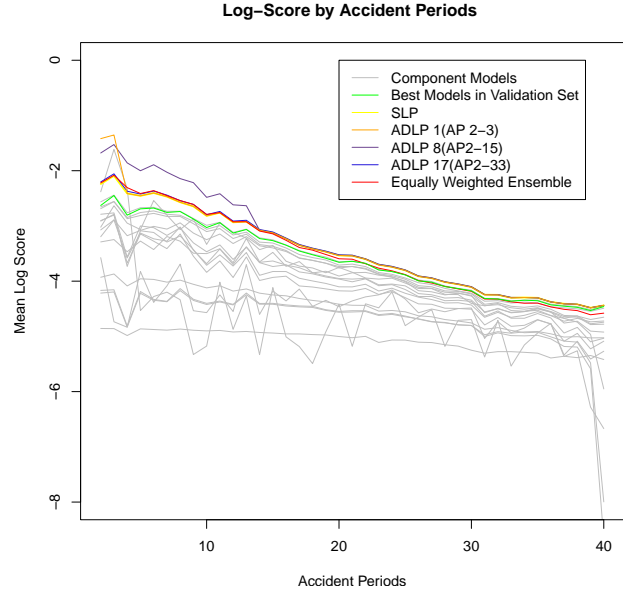


Figure 6.4: Log Score Plot by Accident Periods (higher is better): comparison among different partition strategies

data used in this paper. For practical application, if there is no substantial difference among the performance of component models in earlier accident periods, one may consider simply allocating the first half of accident periods to the first subset.

6.2.3. Analysing the difference in distributional forecast performance using statistical tests

The Log Scores of the ADLP in Figure 6.3 are clearly higher than that of the SLP, but we haven't established whether this difference is statistically significant yet. To analyse the statistical significance of the improvement over the traditional approaches brought by the ADLP ensembles, we run the Diebold-Mariano test and the Adjusted Diebold-Mariano test on each simulated dataset (see (5.4) and (A.4), respectively), with the null hypothesis stating that the two strategies have equal performance. In particular, we test $ADLP_8$, which has the best predictive performance measured by Log Score, against the EW and BMV, respectively. If the null hypothesis is rejected, the $ADLP_8$ should be favoured.

Figure 6.5 illustrates the distribution of test statistics under the Diebold-Mariano test and the Adjusted Diebold-Mariano test, with the red dashed line marking the critical value at the customary 5% significance level. The test statistics above the red dashed line indicate those datasets where the null hypothesis has been rejected, and the number of rejections under each test is summarised in Table 6.1. Since the null hypothesis is rejected for most simulations and almost all the test statistics are above zero (as marked by the blue dashed line), both the DM test and the adjusted DM test imply a decision in favour of $ADLP_8$.

Table 6.1: The Number of Datasets (out of 100) when H_0 is rejected under 5% significance level

Hypothesis Tests	DM Test	Adjusted DM Test
$ADLP_8$ vs EW	94	92
$ADLP_8$ vs BMV	99	84
SLP vs EW	84	81
SLP vs BMV	90	89
$ADLP_8$ vs SLP	82	73

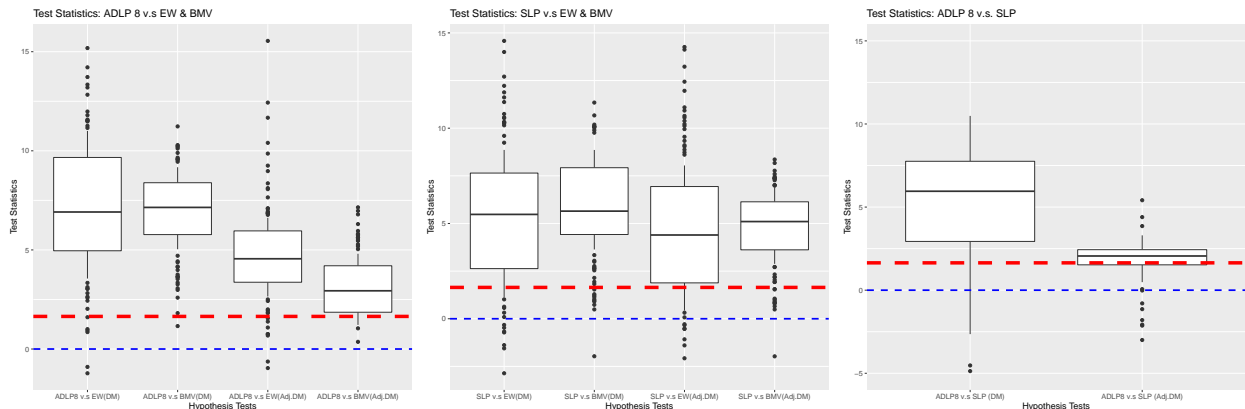


Figure 6.5: Test Statistics: ADLP₈ v.s. EW and BMV Figure 6.6: Test Statistics: SLP v.s. EW and BMV Figure 6.7: Test Statistics: ADLP₈ v.s. SLP

We now investigate where the difference in the performance between ADLP₈ and BMV or the EW comes from. Since we expect the improvement over the traditional approaches to partially come from the ability of linear pools to optimise the combination of component models based on Log Score, firstly, we test the Standard Linear Pool (SLP) against the traditional approaches for each simulated data set. As per Figure 6.6 and Table 6.1, the null hypothesis is rejected for most simulated data sets, and most of the test statistics are positive, SLP is favoured over BMV and the EW by both the DM test and the adjusted DM test in most cases.

As per the discussion in Section 3.5, we expect ADLP₈ to improve SLP by better taking into the typical reserving characteristics found in the simulated data set. Based on the results shown in Table 6.1 and Figure 6.6, ADLP₈ is favoured by the statistical tests in most simulated data sets.

Therefore, the outstanding performance of ADLP₈ can be decomposed into two parts. Firstly, it improves the performance of the model selection strategy and the equally weighted ensemble, which can be credited to the advantages of linear pools in model combination. Secondly, as a linear pool ensemble being specially tailored to the general insurance loss reserving purpose, ADLP₈ further improves the performance of SLP by considering the impact from accident periods and development periods on the ensemble’s performance.

6.3. Comparisons using the CRPS

In the previous subsection, we established the superiority of the ADLP using the Log Score. However, model parameters and model weights were optimised using that same criterion, and one may wonder whether that superiority still holds under a different criterion. The CRPS is also a strictly proper score, and we show in this subsection that it leads to the same ranking of models. Here, the proposed ensembles are evaluated by their CRPS averaging over out-of-sample observations.

We begin by testing whether the ADLP₈ model is still the optimal split. Figure 6.8 illustrates the mean out-of-sample CRPS of ADLP ensembles with different split points. In contrast to the Log Score, one should note that CRPS is a negatively oriented score, meaning a lower score is given to the model with better performance. The grey dot represents the mean CRPS attained by SLP, and the black dot highlights the minimum mean CRPS, which is attained at the accident period 23 and corresponds to ADLP₁₃. The brown dot shows the mean CRPS attained by ADLP₈. The mean CRPS forms a U shape, suggesting the performance of ADLP ensembles increases with the split point before the accident period 23 and deteriorates afterwards. This pattern is generally consistent with the Log Score results, though the best performance is obtained at different accident periods (i.e. the minimum CRPS is achieved using the split point at the accident period 23, whereas the maximum Log Score is obtained using the split point at the accident period 15).

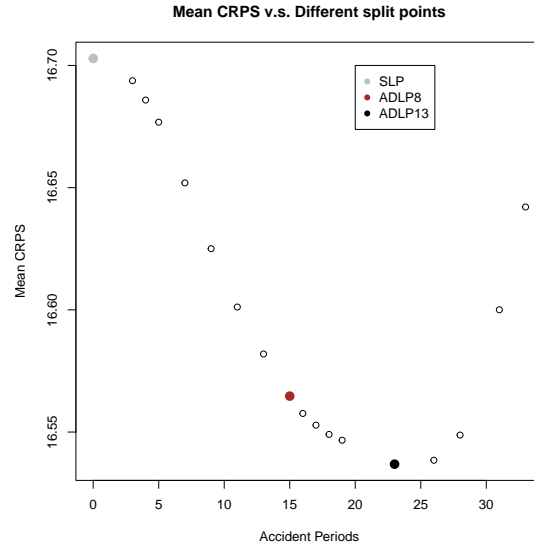


Figure 6.8: Mean CRPS Plot (lower is better): comparison among different partition strategies

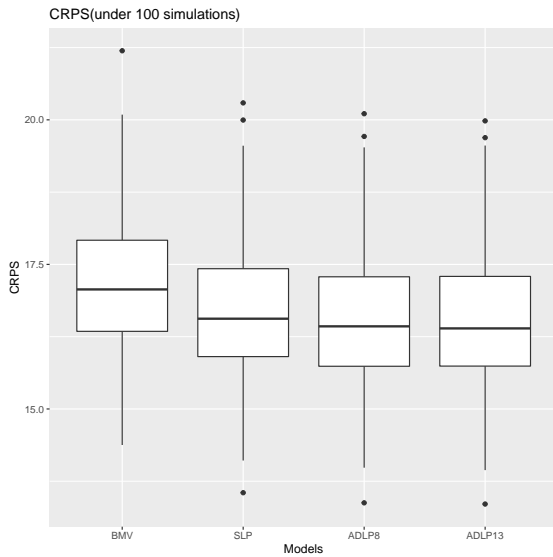


Figure 6.9: Distribution of CRPS over 100 simulations (lower is better): comparison among BMV, SLP, ADLP₈, and ADLP₁₃

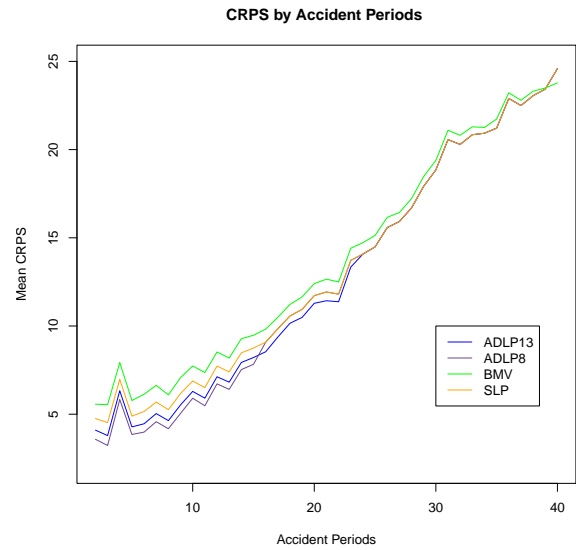


Figure 6.10: Mean CRPS by accident periods (lower is better)

Next, we assess whether the ADLP still outperforms the BMV, EW, and SLP. Figure 6.9 compares the distribution of CRPS attained by BMV, SLP, ADLP₈ and ADLP₁₃ over 100 simulations. ADLP₈ has a lower average CRPS of 16.5647 than both the average CRPS of BMV (17.1784) and the average CRPS of SLP (16.7029), with similar variability in performance. Furthermore, there is no substantial difference between the CRPS of ADLP₈ and ADLP₁₃. In fact the difference does not seem to be statistically significant; see below.

The CRPS attained by BMV, SLP, ADLP₈ and ADLP₁₃ at each accident period are plotted in Figure 6.10. The model selection strategy (i.e. BMV) has the highest CRPS across all accident periods in Figure 6.10. ADLP₈ still has the best performance before the accident period 15 as it has the lowest CRPS in that period. ADLP₁₃ has the lowest CRPS between the accident period 15 and 23. When calculating the CRPS

averaging over accident periods, the outstanding performance of $ADLP_{13}$ between the accident period 15 and 23 might offset its underperformance relative to $ADLP_8$ before the accident period 15.

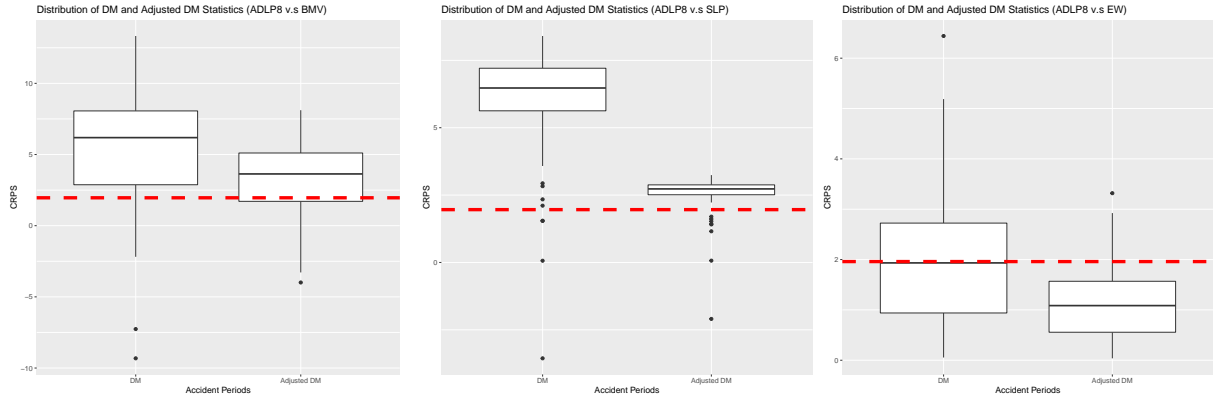


Figure 6.11: Test statistics based on Figure 6.12: Test statistics based on Figure 6.13: Test statistics based on
 CRPS (values above the red dashed CRPS (values above the red dashed CRPS (values above the red dashed
 line reject equal performance): line reject equal performance): line reject equal performance):
 $ADLP_8$ v.s BMV $ADLP_8$ v.s SLP $ADLP_8$ v.s EW

Finally, to formally assess the difference between the CRPS of $ADLP_8$ (i.e. the recommended ADLP ensemble by Log Score) and the basic ensembling strategies (i.e. BMV, EW and SLP), the Diebold-Mariano (DM) and adjusted Diebold-Mariano tests are performed, with the distribution of test statistics being shown in Figure 6.11, Figure 6.13 and Figure 6.12, respectively. The red dashed line marks the critical value at the 5% significance level. As per Figure 6.11, since most test statistics are above the critical value under both the DM and the adjusted DM test, the null hypothesis of equal performance is rejected for most simulated datasets, with a rejection rate of 0.92 under the DM test and 0.83 under the adjusted DM test. Therefore, both tests imply a decision in favour of $ADLP_8$ relative to BMV. Similarly, the null hypothesis of equal performance between $ADLP_8$ and SLP is also rejected for most simulated datasets based on Figure 6.12, with a rejection rate of 0.96 under the DM test and 0.92 under the adjusted DM test. However, as per Figure 6.13, the null hypothesis of equal performance between $ADLP_8$ and the equally weighted ensemble is only rejected in 50 simulated datasets under the DM test and 13 simulated datasets under the adjusted DM test. Compared with other evaluation metrics, the equally weighted ensemble performs better under CRPS. The characteristics of CRPS might provide some explanation for this phenomenon. As per Gneiting and Raftery (2007) and Schneider, Henriksen and Stisen (2020), CRPS is less sensitive to outliers and extreme cases and generally places less penalty on large errors with relatively small probabilities. Therefore, although each component model receives an equal weight, a few poor-performing models tend to have a relatively small impact on the equally weighted ensemble's CRPS. In contrast, for other evaluation metrics, such as the reserve bias at the 75th quantile, an extremely poor performing model can easily distort the performance of the equally weighted ensemble. Since the equally weighted ensemble perform poorly based on all other metrics (i.e. Log Score, central reserve bias and the reserve bias at the 75th quantile) and insurers are also concerned with the tail events, we might still prefer $ADLP_8$ even though the CRPS results are not statistically significant for most simulated datasets.

To evaluate the difference between the CRPS of the best ADLP ensemble identified by the Log Score (i.e. $ADLP_8$) and the best ADLP ensemble based on CRPS (i.e. $ADLP_{13}$), the test statistics based on the DM and the adjusted DM test are calculated and shown in Figure 6.14. Since most test statistics fail to pass the critical value, the null hypothesis cannot be rejected for the majority of simulated data sets. In fact, the rejection rate is only 0.34 under the DM test and 0.01 under the adjusted DM test. Therefore, although $ADLP_{13}$ has a slightly lower CRPS averaging over 100 simulations than $ADLP_8$, there is insufficient evidence for us to conclude $ADLP_{13}$ outperforms $ADLP_8$ based on CRPS. Additionally, in later sections, we have also shown that $ADLP_8$ outperforms $ADLP_{13}$ based on the central reserve bias and reserve bias at the 75th

quantile. Therefore, on the whole, we recommend $ADLP_8$ be used.

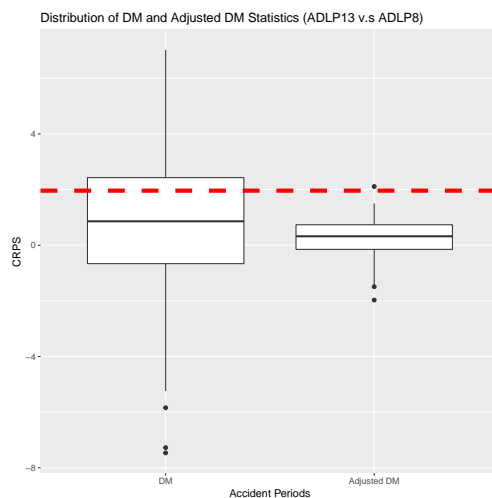


Figure 6.14: Test statistics based on CRPS (values above the red dashed line reject equal performance): $ADLP_8$ v.s $ADLP_{13}$

6.4. Predictive performance on aggregate reserve level

The average relative central bias and the 75th reserve bias calculated following the methodology specified in Section 5.4 for all methods are summarised in Figure 6.15 and Figure 6.16, respectively. Since the relative 75th quantile of reserve bias for the equally weighted ensemble (i.e. 19.21%) is significantly larger than others methods, we do not display it on the graph.

As per Figure 6.15, all ADLP ensembles, including SLP as a special case, yield more accurate central estimates of the reserves than the BMV and the EW. The performance of ADLP ensembles increases with the split points before accident period 15 and deteriorates afterwards. This pattern is in line with our findings in Figure 6.3. Hence, $ADLP_8$, which has the highest average Log Score on incremental claims level, retains its top performance on central reserve estimation.

In terms of reserve quantile estimation, all ADLP ensembles outperform the equally weighted ensemble, which has an absolute relative bias of 0.1921. To avoid the distortion of scales, the absolute relative reserve bias for the equally weighted ensemble is not shown in Figure 6.16. However, not all ADLP ensembles outperform the BMV, and the pattern of ensembles' performance shown in Figure 6.16 is not as clear as either Figure 6.15 or Figure 6.3. This phenomenon might be explained by the higher uncertainty involved in simulating reserve quantiles from ensembles. As shown in Section 4.2, to generate a random variable from any ensemble, a uniform random variable is firstly simulated to determine from which component model a random variable is generated. This additional simulation step may increase the uncertainty of reserve quantile estimation by ensembles. Also, the “true” quantiles are estimated from a sample of 100 values only, and are hence quite volatile, too. Despite the variability present in the plot, the relationship between ADLP ensembles' performance and split points is generally consistent with the pattern found in Figure 6.15. Although $ADLP_8$ does not yield the smallest reserve bias at 75th quantile, the minimum is still attained near accident period 15. Therefore, using any split point between accident period 15 and accident period 20 can still yield satisfactory performance at the 75th reserve quantile, and we are confident the corresponding ADLP ensembles can still substantially outperform the BMV.

6.5. Analysis of optimal model weights

Analyzing the combination weights can potentially help modelers gain insights about the component models' properties, and examples can be found in (Taylor, 2000) and (Kessy, Sherris, Villegas and Ziveyi,

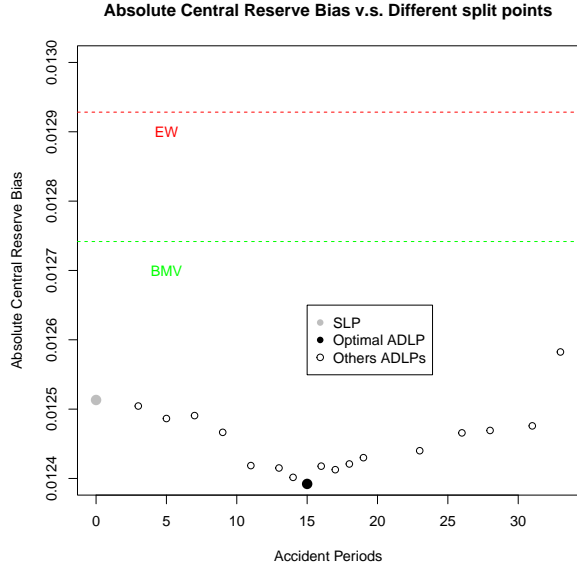


Figure 6.15: Absolute Central Relative Reserve Bias

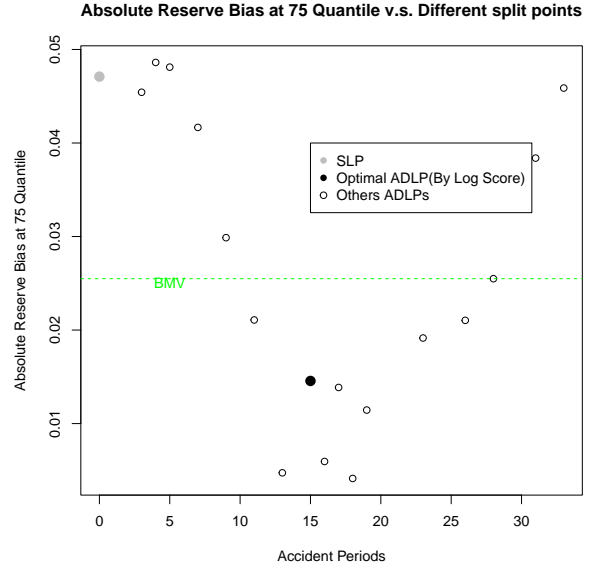


Figure 6.16: Absolute Relative Reserve Bias at 75th Quantile

2021). Therefore, we extract the combination weights from ADLPs, with Figure 6.17 plotting the model weights in subset 1 using different split points, and Figure 6.18 illustrating the model weights in subset 2. Since model weights under ADLPs in the second subset are trained using the whole validation data—remember (3.6), they will be identical to the combination weights under the SLP.

Several models might be worth highlighting. The weight allocated to SP_{LN} , which is the BMV (identified as the model with the highest Log Score **averaging** over different accident periods) in this example, is increasing with the split point as shown in Figure 6.17. Since the combination weights reflect the relative validation performance of component models in the ensemble, SP_{LN} tends to have better performance in more recent accident periods as its weight increases when data from later accident periods are added to the validation set. Indeed, as per Figure 6.18, SP_{LN} is allocated with the largest weight in the second subset. Similar pattern can also be found in the weight assigned to $GAMLSS_{LN}$. However, the weight allocated to GLM_{PPCF} has demonstrated an opposite pattern: there is a substantial weight given to GLM_{PPCF} with the earliest split point, whereas the weight decreases to a small value as the split point increases. This phenomenon might be explained by the ability of GLM_{PPCF} to capture claims finalisation information. Since claims in earlier accident periods are close to being finalised, GLM_{PPCF} tends to yield better predictive performance in earlier accident periods by taking this factor into account. This property of PPCF models has also been noted in (Taylor, 2000).

Besides analysing individual models, we also analyse the weights' pattern at the group level by clustering the component models based on their structure and distributional assumptions. In terms of model structure, all models with standard cross-classified structures are assigned with zero or small weights based in Figure 6.17 and Figure 6.18. Due to the relatively complex characteristics of the simulated data, the standard cross-classified models tend to perform poorly as they only consider the accident and development period effects. We have also found that only one of them will be allocated with a large weight for those models with similar structures. In fact, the models with the four largest weights in both Figure 6.17 and Figure 6.18 all have different structures. This finding highlights the advantage of using linear pools as the weights of potential correlated models can be shrunk towards zero by imposing the non-negativity constraint on weights.

From the angle of distributional assumptions, all models with ODP distributional assumptions are assigned relatively small weights, whereas models with Log-Normal distributional assumptions are allocated

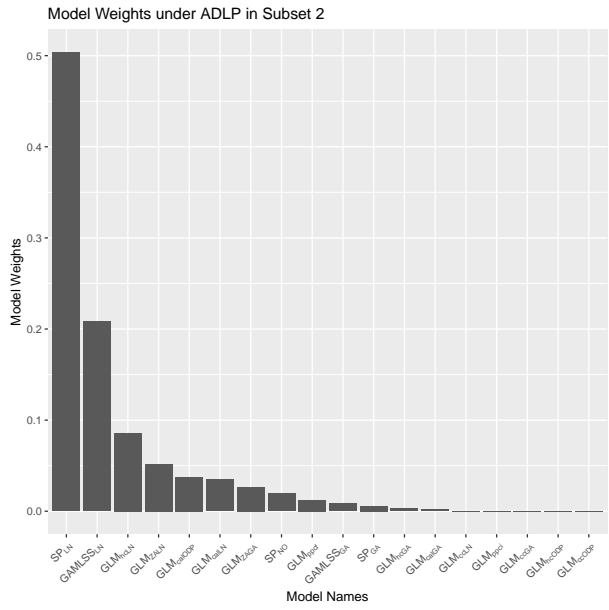
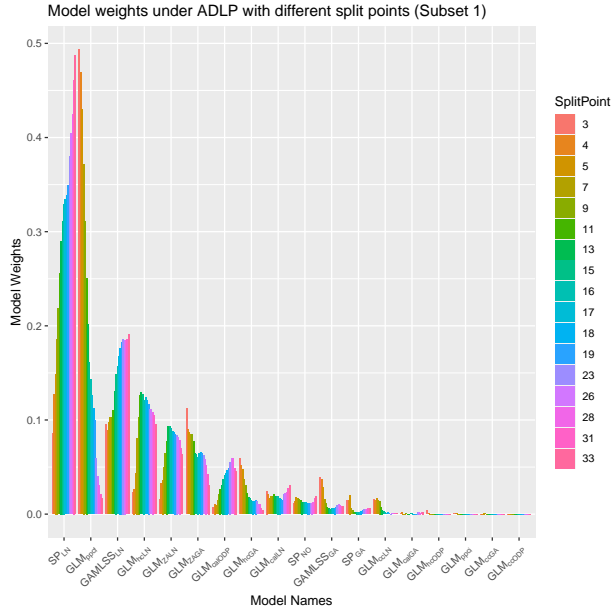


Figure 6.17: Combination Weights in Subset 1: ADLP ensembles Figure 6.18: Combination Weights in SLP and Subset 2 of ADLP

larger weights. Due to the relatively large tail-heaviness of incremental claims’ distribution, Log-Normal tends to provide a better distributional fit as it has a heavier tail than the ODP distribution. Additionally, we have also found that Zero-Adjusted Gamma distribution (ZAGA) is assigned with a larger weight when the split occurs earlier as shown in Figure 6.17. The weight allocation might be explained by the tendency for a greater proportion of zero incremental claims in earlier accident periods as the claims from earlier accident periods are usually closer to their maturity: these are the ones that are the most likely to have 0 claims in the very late development periods (the later accident years haven’t reached that stage in the training set). Since the design of the ZAGA model allows the probability mass of zero incremental claims to be modeled as a function of development periods (i.e., the closeness of claims to their maturity), ZAGA tends to yield better performance on when only the most mature accident periods are used. Interestingly, Zero-Adjusted Log-Normal (ZALN) model has been assigned with small weights for earlier accident periods splits, which might be explained by the fact that it tends to be redundant with ZAGA.

Remark 6.1. *Due to the increased flexibility offered by statistical models, one might argue a single model can capture most of the possible features through careful model design, or simply advocate the use of the model with the highest weight. However, this attempt might lead to poorer performance out-of-sample. In Appendix C.3, we provide a simple example to illustrate this idea.*

As per Figure 6.18, SP_{LN} and $GAMLSS_{LN}$ constitute nearly 70% of total combination weights due to their outstanding performance. In the example shown in Appendix C.3, we explore whether a new model built by integrating the structures of both SP_{LN} and $GAMLSS_{LN}$ can out-perform SP_{LN} , which is the best model in the validation set. Although the new model, denoted as $GAMLSS_{LN}^{SP}$, receives a higher training Log Score than SP_{LN} , it under-performs SP_{LN} in out-of-sample data. The results imply that when we design a model with the hope of capturing all the data characteristics, such an attempt might lead to over-fitting as not every feature has the same level of impact on the incremental claims. We further compare the performance of a standard linear pool build from SP_{LN} and $GAMLSS_{LN}$ with $GAMLSS_{LN}^{SP}$. Not surprisingly, the SLP generates a higher (out-of-sample) Log Score than both SP_{LN} and $GAMLSS_{LN}^{SP}$. Therefore, when multiple patterns are present in the loss reserving data, linear pools might offer a better solution as it allows the data to determine the weights allocated to various models depending on the strength of information for different model specifications.

7. Conclusions

In this paper, we have designed, constructed, analysed and tested an objective, data-driven method to optimally combine different models for reserving. Using the Log Score as the combination criterion, the proposed ensemble modelling framework has demonstrated its potential in yielding high distributional forecast accuracy.

Although the standard ensembling approach (e.g. the standard linear pool) has demonstrated success in non-actuarial fields, it does not yield the optimal performance in the loss reserving context considered in this paper. To address the common general insurance loss data characteristics as listed in Section 1.2, we introduced the **Accident and Development period adjusted Linear Pools (ADLP)** modelling framework. This includes a novel validation strategy that takes account into the triangular loss reserving data structure, impacts and features related to different Accident and Development period combinations.

In particular, the partitioning strategy not only effectively utilises variations in component models' performance in different accident periods, but also captures the impact from late development periods on incremental claims, which can be particularly important for long-tailed lines of insurance business. Based on the illustrative examples which use simulated aggregate loss reserving data, the ADLP ensembles outperform traditional approaches (i.e., the model selection strategy BMV and the equally weighted ensemble EW) and the standard linear pool ensemble, when the Log Score, CRPS, or relative reserve bias are used for the assessment.

Furthermore, we also investigate the impact of a split point on the ensemble's performance. Given the composition of models included in the ensemble, we have found that splitting data into two subsets close to the middle point (i.e., between accident period 15 and 20 for a 40 x 40 loss triangle) can generally yield satisfactory performance by taking the advantages of several high-performing models in earlier accident periods while maintaining sufficient data size for training the combination weights in the both subsets.

Acknowledgements

Earlier versions of this paper were presented at the Actuaries Institute 2022 All Actuaries Summit, as well as at the One World Actuarial Research Seminars. The authors are grateful for constructive comments received from colleagues who attended those events.

This research was supported under Australian Research Council's Discovery Project funding scheme (DP200101859). The views expressed herein are those of the authors and are not necessarily those of the supporting organisations.

Data and Code

All data sets were generated using the CRAN package `Synthetic` as explained above. All other relevant codes can be found at <https://github.com/agi-lab/reserving-ensemble>.

Declarations of interest

None

References

References

- Aiolfia, M., Timmermann, A., 2006. Persistence in forecasting performance and conditional combination strategies. *Journal of Econometrics* 135, 31–53.
- Al-Mudafer, M.T., Avanzi, B., Taylor, G.C., Wong, B., 2022. Stochastic loss reserving with mixture density neural networks. *Insurance: Mathematics and Economics* in press.
- APRA, 2019. Prudential standard gps 340 insurance liability valuation. <https://www.legislation.gov.au/Details/F2018L00738>.

- Avanzi, B., Taylor, G., Wang, M., Wong, B., 2021a. Synthetic: an individual insurance claim simulator with feature control. *Insurance: Mathematics and Economics* .
- Avanzi, B., Taylor, G., Wang, M., Wong, B., 2021b. SynthETIC: Synthetic experience tracking insurance claims. <https://CRAN.R-project.org/package=SynthETIC>.
- Baars, J.A., Mass, C.F., 2005. Performance of national weather service forecasts compared to operational, consensus, and weighted model output statistics. *Weather and Forecasting* 20, 1034–1047.
- Bellman, R., 1966. Dynamic programming. *Science* 153, 34–37.
- Bjørnland, H.C., Gerdrup, K., Jore, A.S., Smith, C., Thorsrud, L.A., 2011. Weights and pools for a norwegian density combination. *The North American Journal of Economics and Finance* 22, 61–76.
- Breiman, L., 1996. Stacked regressions. *Machine learning* 24, 49–64.
- Claeskens, G., Magnus, J.R., Vasnev, A.L., Wang, W., 2016. The forecast combination puzzle: A simple theoretical explanation. *International Journal of Forecasting* 32, 754–762.
- Conflitti, C., De Mol, C., Giannone, D., 2015. Optimal combination of survey forecasts. *International Journal of Forecasting* 31, 1096–1103.
- Coqueret, G., Guida, T., 2020. *Machine Learning for Factor Investing: R Version*. CRC Press.
- Diebold, F.X., Mariano, R.S., 1995. Comparing predictive accuracy. *Journal of Business and Economic Statistics* 13, 253–263.
- Diebold, F.X., Mariano, R.S., 2002. Comparing predictive accuracy. *Journal of Business & economic statistics* 20, 134–144.
- England, P.D., Verrall, R.J., 2001. A flexible framework for stochastic claims reserving, in: *Proceedings of the Casualty Actuarial Society*, pp. 1–38.
- Friedland, J., 2010. Estimating unpaid claims using basic techniques. *Casualty Actuarial Society* .
- Gabrielli, A., 2020. A neural network boosted double overdispersed poisson claims reserving model. *ASTIN Bulletin: The Journal of the IAA* 50, 25–60.
- Gneiting, T., Katzfuss, M., 2014. Probabilistic forecasting. *Annual Review of Statistics and Its Application* 1, 125–151.
- Gneiting, T., Raftery, A.E., 2007. Strictly proper scoring rules, prediction, and estimation. *Journal of the American Statistical Association* 102, 359–378.
- Gneiting, T., Raftery, A.E., Westveld III, A.H., Goldman, T., 2005. Calibrated probabilistic forecasting using ensemble model output statistics and minimum crps estimation. *Monthly Weather Review* 133, 1098–1118.
- Gneiting, T., Ranjan, R., 2011. Comparing density forecasts using threshold-and quantile-weighted scoring rules. *Journal of Business & Economic Statistics* 29, 411–422.
- Gneiting, T., Ranjan, R., et al., 2013. Combining predictive distributions. *Electronic Journal of Statistics* 7, 1747–1782.
- Good, I.J., 1992. Rational decisions, in: *Breakthroughs in statistics*. Springer, pp. 365–377.
- Green, P.J., Silverman, B.W., 1993. *Nonparametric regression and generalized linear models: a roughness penalty approach*. Crc Press.
- Gu, C., Xiang, D., 2001. Cross-validating non-gaussian data: generalized approximate cross-validation revisited. *Journal of Computational and Graphical Statistics* 10, 581–591.
- Hall, S.G., Mitchell, J., 2004. Density forecast combination. *Tanaka Business School*.
- Hall, S.G., Mitchell, J., 2007. Combining density forecasts. *International Journal of Forecasting* 23, 1–13.
- Hersbach, H., 2000. Decomposition of the continuous ranked probability score for ensemble prediction systems. *Weather and Forecasting* 15, 559–570.
- Jamal, S., Canto, S., Fernwood, R., Giancaterino, C., Hiabu, M., Invernizzi, L., Korzhynska, T., Martin, Z., Shen, H., 2018. Machine learning & traditional methods synergy in non-life reserving. Report of the ASTIN Working Party of the International Actuarial Association. Available online: https://www.actuaries.org/IAA/Documents/ASTIN/ASTIN_MLTMS%20Report_SJAMAL.pdf (accessed on 19 July 2019) .
- Kessy, S., Sherris, M., Villegas, A., Ziveyi, J., 2021. Mortality forecasting using stacked regression ensembles. Available at SSRN 3823511 .
- Kuo, K., 2019. Deeptriangle: A deep learning approach to loss reserving. *Risks* 7, 97.
- Mack, T., 1991. A simple parametric model for rating automobile insurance or estimating ibnr claims reserves. *ASTIN Bulletin: The Journal of the IAA* 21, 93–109.
- Mack, T., 1993. Distribution-Free Calculation of the Standard Error of Chain Ladder Reserve Estimates. *ASTIN Bulletin* 23, 213–225.
- McDonald, C., Thorsrud, L.A., et al., 2011. Evaluating density forecasts: model combination strategies versus the RBNZ. Technical Report. Reserve Bank of New Zealand.
- Opschoor, A., Van Dijk, D., Van der Wel, M., 2017. Combining density forecasts using focused scoring rules. *Journal of Applied Econometrics* 32, 1298–1313.
- Parry, M., Dawid, A.P., Lauritzen, S., 2012. Proper local scoring rules. *The Annals of Statistics* 40, 561–592.
- Pinar, M., Stengos, T., Yazgan, M.E., 2012. Is There an Optimal Forecast Combination?: A Stochastic Dominance Approach to the Forecasting Combination Puzzle. Department of Economics and Finance, College of Management and Economics .
- Raftery, A.E., Gneiting, T., Balabdaoui, F., Polakowski, M., 2005. Using bayesian model averaging to calibrate forecast ensembles. *Monthly weather review* 133, 1155–1174.
- Ranjan, R., Gneiting, T., 2010. Combining probability forecasts. *Journal of the Royal Statistical Society: Series B (Statistical Methodology)* 72, 71–91.
- Renshaw, A.E., Verrall, R.J., 1998. A stochastic model underlying the chain-ladder technique. *British Actuarial Journal* 4, 903–923.
- Resti, Y., Ismail, N., Jamaan, S.H., 2013. Estimation of claim cost data using zero adjusted gamma and inverse gaussian regression models. *Journal of Mathematics and Statistics* 9, 186–192.

- Rigby, R.A., Stasinopoulos, D.M., 2005. Generalized additive models for location, scale and shape. *Journal of the Royal Statistical Society: Series C (Applied Statistics)* 54, 507–554.
- Roulston, M.S., Smith, L.A., 2002. Evaluating probabilistic forecasts using information theory. *Monthly Weather Review* 130, 1653–1660.
- Schneider, R., Henriksen, H.J., Stisen, S., 2020. A robust objective function for calibration of groundwater models in light of deficiencies of model structure and observations. *Hydrology and Earth System Sciences Discussions* , 1–26.
- Shapland, M.R., 2022. Using the hayne mle models: A practitioner’s guide. *CAS Monograph* 4.
- Smith, J., Wallis, K.F., 2009. A simple explanation of the forecast combination puzzle. *Oxford Bulletin of Economics and Statistics* 71, 331–355.
- Spedicato, G.A., Clemente, A.G.P., Schewe, F., 2014. The use of gamlss in assessing the distribution of unpaid claims reserves, in: *Casualty Actuarial Society E-Forum, Summer 2014-Volume 2*.
- Taylor, G., 2000. *Loss Reserving: An Actuarial Perspective*. Huebner International Series on Risk, Insurance and Economic Security, Kluwer Academic Publishers.
- Taylor, G.C., McGuire, G., 2016. Stochastic loss reserving using Generalized Linear Models. *Casualty Actuarial Society*.
- Taylor, G.C., Xu, J., 2016. An empirical investigation of the value of finalisation count information to loss reserving. *Variance* in press.
- Verrall, R.J., 1991. On the estimation of reserves from loglinear models. *Insurance: mathematics and economics* 10, 75–80.
- Vogel, P., Knippertz, P., Fink, A.H., Schlueter, A., Gneiting, T., 2018. Skill of global raw and postprocessed ensemble predictions of rainfall over northern tropical africa. *Weather and Forecasting* 33, 369–388.
- Wright, T.S., 1990. A stochastic method for claims reserving in general insurance. *Journal of the Institute of Actuaries* 117, 677–731.
- Wüthrich, M.V., 2018. Neural networks applied to chain–ladder reserving. *European Actuarial Journal* 8, 407–436.
- Wüthrich, M.V., Merz, M., 2008. *Stochastic claims reserving methods in insurance*. John Wiley & Sons, Chichester.
- Yao, Y., Vehtari, A., Simpson, D., Gelman, A., 2018. Using stacking to average bayesian predictive distributions (with discussion). *Bayesian Analysis* 13, 917–1007.

A. Distributional forecasting concepts

A.1. Log Score and Kullback-Leibler Divergence Distance

The Log Score has a close connection to the Kullback-Leibler divergence (KLIC) distance between the true density f_m and the predicted density \hat{f}_m (Hall and Mitchell, 2007), which is defined as:

$$\text{KLIC} = \ln(f_m(y_{ij})) - \ln(\hat{f}_m(y_{ij})) \quad (\text{A.1})$$

The smaller the KLIC distance, the smaller the deviation of the predictive density from the true density. If the predictive density is equal to the true density, its KLIC distance will be zero. However, direct minimization of the difference between the true density and the predictive density might not be feasible, as the true density is often unknown in practice. One solution is to maximise $\ln(\hat{f}_m(y_{ij}))$, which is equivalent to minimise the KLIC distance (Hall and Mitchell, 2007). As $\ln(\hat{f}_m(y_{ij}))$ corresponds to the Log Score of the predictive density, the logarithmic scoring rule has the nice interpretation of assigning a higher score to the predictive density with a closer distance to the true density (Hall and Mitchell, 2007).

A.2. Interpretation of the CRPS

The CRPS can be interpreted as a measurement of the difference between the predicted and observed cumulative distributions (Hersbach, 2000). Another interpretation of CRPS is given by Bjørnland, Gerdrup, Jore, Smith and Thorsrud (2011). The ideal perfect forecaster should assign a probability mass of one to the materialized events, which corresponds to the cumulative distribution function

$$I_{z \geq y_k} = \begin{cases} 1 & \text{if } z \geq y_k; \\ 0 & \text{if } z < y_k. \end{cases}$$

Therefore, the CRPS can be interpreted as a measurement of the deviation of a predictive distribution from the perfect forecast distribution, and the minimum value of CRPS under perfect forecasting can be attained if $F_k(z) = I_{z \geq y_k}$ (i.e. the predictive distribution is equal to the true distribution). Note that CRPS is a negatively oriented score (i.e. better performance is indicated by a lower CRPS value).

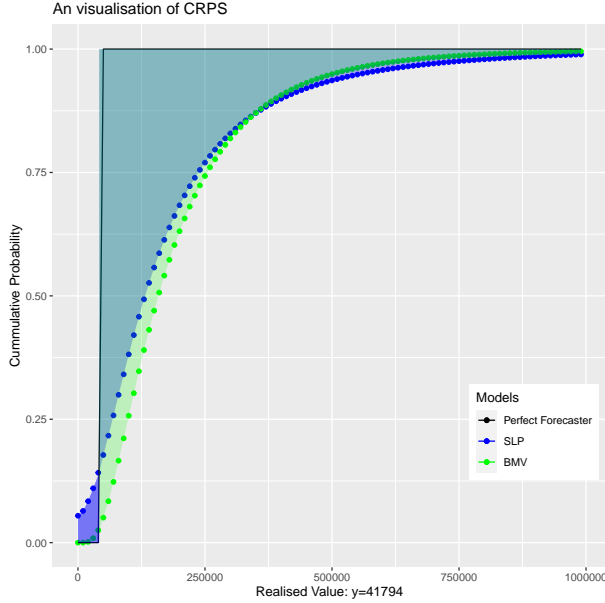


Figure A: A visualisation of CRPS

For an ensemble forecast F^* , the CRPS at observation y_k can be expressed as:

$$\text{CRPS}(F^*, y_k) = \int_{-\infty}^{\infty} \left(\sum_{m=1}^M w_m \cdot F_m(y_k) - \mathbb{I}_{z \geq y_k} \right)^2 dz. \quad (\text{A.2})$$

Since an ensemble usually includes models from different distributional classes, there is no closed-form expression for the CRPS of the ensemble. Therefore, the CRPS for ensemble forecasts is usually approximated by its discretised version (Gneiting and Ranjan, 2011)

$$\text{CRPS}(F^*, y_k) = \sum_{z=z_l}^{z_u} \left(\sum_{m=1}^M w_m \cdot F_m(y_k) - \mathbb{I}_{z \geq y_k} \right)^2, \quad (\text{A.3})$$

where z_l and z_u are the lower and upper bounds for integration, respectively. We can then take the average of CRPS over the out-of-sample observations $y_1, y_2, \dots, y_{|D_{out}|}$ to evaluate a model's performance.

Figure A illustrates CRPS at a realised incremental claim value. The black line represents the perfect forecaster, which only assigns a probability mass of 1 to the realised value. The (discretised) Cumulative Distribution Function (CDF) of SLP and BMV are represented by the blue and green points, respectively. The CRPS is then the sum of the squared distance between the forecaster's CDF and the CDF of the perfect forecaster. For visualisation purposes, Figure A shows the absolute distance instead, with the blue shaded area showing the sum of absolute distance between SLP's CDF and the perfect forecaster's CDF and the green shaded area representing the sum of absolute distance between BMV's CDF and the CDF of the perfect forecaster. At $y = 41794$, the calculated CRPS for SLP is 5.9808, which is lower than the BMV's CRPS of 8.1061.

A.3. Adjusted Diebold-Mariano Test

Diebold and Mariano (2002) suggests the original Diebold-Mariano test might not work well under the serial correlation and contemporaneous correlation. Serial correlation can occur due to the time-series characteristics of incremental claims data. Contemporaneous correlation refers to the correlation between the score of two competing models, which can occur as the two models are predicting the same data. In light

of the above issues, Diebold and Mariano (2002) proposes an adjusted version of the DM Test by taking into account both the contemporaneous correlation and the serial correlation.

Denote d_{ij} as the Log Score differential between the two competing forecast at point y_{ij} (i.e. $d_{ij} = \ln(\widehat{f}_F(y_{i,j})) - \ln(\widehat{f}_G(y_{i,j}))$) and \bar{d} denote the mean Log Score differential between the two forecasters. We further denote $f_d(0)$ as the spectral density of loss differential at frequency zero with $f_d(0) = \sum_{\tau=-\infty}^{\infty} \gamma_d(\tau)$, where $\gamma_d(\tau)$ is the auto-covariance function: $\gamma_d(\tau) = E[(d_{ij} - \mu)(d_{i-\tau,j-\tau} - \mu)]$ with $\mu = E[d_{ij}]$. According to Diebold and Mariano (2002), the adjusted DM test statistic is:

$$S_1 = \frac{\bar{d}}{\sqrt{\frac{\widehat{f}_d(0)}{|D_{out}|}}} \sim N(0, 1) \quad (\text{A.4})$$

where $\sqrt{\frac{\widehat{f}_d(0)}{|D_{out}|}}$ is an estimation of the variance of the mean score differential. Diebold and Mariano (2002) argues that the spectral density of loss differential at frequency zero provides a more appropriate estimation of the variance of the mean score differential than $\hat{\sigma}_n^2$ by adjusting for serial correlation and contemporaneous correlation. Similarly, as the original Diebold-Mariano, the null hypothesis will be rejected at the significance level of 5% if $S_1 > z_{1-\alpha}$.

B. Technical details

B.1. Details of Calculating Reserve Quantiles

To simulate the 75th reserve quantile for component model m , we implement the following procedure:

- 1. Simulate N random variables for each cell in out-of-sample data from its corresponding distribution; Denote $\tilde{Y}_{ij}^m = (\tilde{Y}_{ij,(1)}^m, \tilde{Y}_{ij,(2)}^m, \dots, \tilde{Y}_{ij,(N)}^m)$ as the vector of all simulated random variables for cell (i,j) under the component model m
- 2. Repeat Step 1 for each cell (i, j)
- 3. Calculate the simulated reserve based on the simulated random variables for each cell (i, j) : $\tilde{R}^m = (\tilde{R}_{(1)}^m, \tilde{R}_{(2)}^m, \dots, \tilde{R}_{(N)}^m) = (\sum_{i,j \in D^{out}} \tilde{Y}_{ij,(1)}^m, \sum_{i,j \in D^{out}} \tilde{Y}_{ij,(2)}^m, \dots, \sum_{i,j \in D^{out}} \tilde{Y}_{ij,(N)}^m)$
- 4. Calculate the empirical 75th quantile of the N simulated reserves for component model m : R_{75}^m

Here we take $N = 1000$, which provides enough to be computationally feasible but also reasonably accurate at the quantiles we are looking at. One should also note that the above simulation procedure implicitly assumes the independence of individual cells, which is a common assumption used to simulate reserve quantiles in literature (Gabrielli, 2020). The procedure mentioned above is similar to the parametric bootstrapping method of simulating reserve (Taylor and McGuire, 2016). Since this paper focuses on assessing predictive distributions, we do not pursue non-parametric or semi-parametric bootstrapping further here.

B.2. Constraints on Combination Weights: Acting as Downside Insurance

As Breiman (1996) suggests, imposing the sum-to-unity and non-negativity constraints act as downside insurance for the out-of-sample predictive performance of the ensemble. This proposition can be supported by the following simple proof.

Denote $\hat{f}^*(y_{ij}) = \sum_{m=1}^M w_m \hat{f}_m(y_{ij})$ as the predictive density for the ensemble at out-of-sample point y_{ij} , and $\hat{f}_{worst}(y_{ij}) = \min\{\hat{f}_m(y_{ij}), m = 1, \dots, M\}$ as the the lowest predictive density at the same data point from one of the component model m (i.e. the predictive density from the worst component model). By imposing the sum-to-unity constraint and non-negativity constraints on model weights, $\ln(\sum_{m=1}^M w_m \hat{f}_m(y_{ij})) \geq \ln(\hat{f}_{worst}(y_{ij}))$ is guaranteed.

B.3. Proof of Lemma 4.1

Proof of Lemma 4.1.

$$\begin{aligned}\mu_{ij}^* &= \int_{-\infty}^{\infty} y_{ij} \cdot f^*(y_{ij}) dy_{ij} = \int_{-\infty}^{\infty} y_{ij} \cdot \sum_{m=1}^M w_m f_m(y_{ij}) dy_{ij} = \sum_{m=1}^M w_m \int_{-\infty}^{\infty} y_{ij} f_m(y_{ij}) dy_{ij} \\ &= \sum_{m=1}^M w_m \cdot \mu_{ij}^m\end{aligned}\tag{B.1}$$

□

B.4. Proof of Lemma 4.2

Proof of Lemma 4.2. Because $U \sim \text{Uniform}(0, 1)$ then $F(U \leq u) = u$. Therefore,

$$\Pr\left(\sum_{m=1}^{l-1} w_m < U < \sum_{m=1}^l w_m\right) = F\left(\sum_{m=1}^l w_m\right) - F\left(\sum_{m=1}^{l-1} w_m\right) = \sum_{m=1}^l w_m - \sum_{m=1}^{l-1} w_m = w_l\tag{B.2}$$

as required.

□

C. Additional fitting results

C.1. ADLP with Three Subsets

The average out-of-sample Log Score attained by the four ADLP⁺ ensembles, in comparison with the corresponding ADLP ensembles, are summarised in Table A. The ‘‘Split Points’’ column shows the accident period(s) where the split of subsets occurs for both ADLP ensembles (outside the bracket) and ADLP⁺ ensembles (inside the bracket). As per Table A, the average Log Score differential between the ADLP and the ADLP⁺ ensembles tend to be small, except for ADLP₂ and ADLP₂⁺.

Additionally, based on the box-plot of Log Score in Figure A, the distributions of Log Score for the ADLP and ADLP⁺ over the 100 simulations are also similar, though ADLP₂ under-performs ADLP₂⁺ in most simulated data set by a small margin. The out-performance of ADLP₂⁺ might be explained by the fact that it splits the second and the third subset at accident period 15, which is the ‘‘optimal’’ split point for ADLP ensembles in this example. In fact, ADLP₂⁺ yields a similar performance as ADLP₈, which uses accident period 15 as the split point for its two subsets. Therefore, instead of dividing the data into three subsets, using two subsets to train the model weights with a split point at accident period 15 seems sufficient.

Table A: Comparison of Average Log Score: ADLP v.s. ADLP⁺

Split Points	Average Log Score (ADLP)	Average Log Score (ADLP ⁺)
AP5(AP5 and 15)	-3.8802	-3.8481
AP15(AP15 and 29)	-3.8471	-3.8367
AP17(AP17 and 31)	-3.8476	-3.8406
AP23(AP23 and 33)	-3.8549	-3.8525

The similar performance of ADLP and ADLP⁺ ensembles can also be shown in Figure B, which plots the average Log Score received by ADLP₈ and ADLP₈⁺ at each accident period. Although ADLP₈⁺ has an additional split point at accident period 29, its performance is still analogous to ADLP₈ even after the accident period 15. This phenomenon might be explained by the small variability in component models’ performance after accident period 20, as shown in Figure B, making it difficult for ensembles to exploit the diversity in models’ performance. Therefore, at least for the data set used in this study, there is no

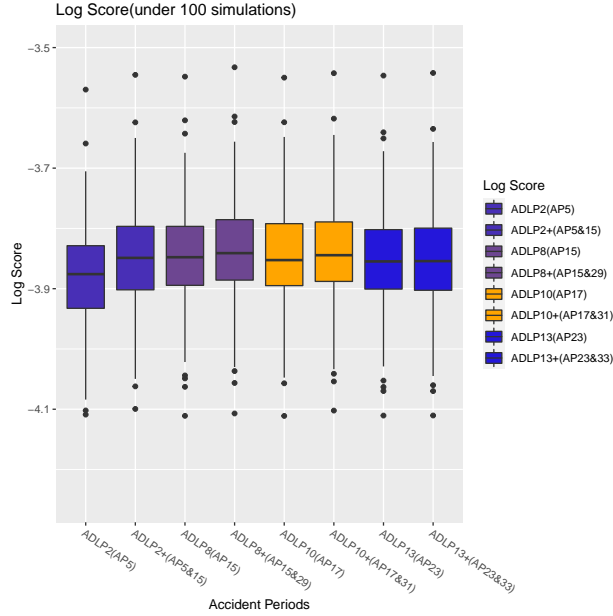


Figure A: Box-plot of Log Score: ADLP v.s. ADLP⁺

substantial improvement in the ensemble’s predictive performance by introducing another subset for training the combination weights.

As per Table A, ADLP₈⁺ has the highest Log Score among all ADLP ensembles with three subsets, and ADLP₈ yields the best performance among the two-subsets ADLP ensembles. We also test whether the Log Score differential between those two partition strategies is statistically significant. The null hypothesis of equal performance is only rejected in 14 out of 100 simulated datasets using the adjusted Diebold-Mariano test. Under the 5% significance level, the rejection rate is considered low. Since ADLP₈⁺ is the best ADLP⁺ ensembles based on Log Score, the test results also imply any other three-subsets partition strategy cannot statistically significantly improve ADLP₈, which is our suggested ADLP ensemble. Additionally, we also feel parsimony would suggest restricting ourselves to a single split point.

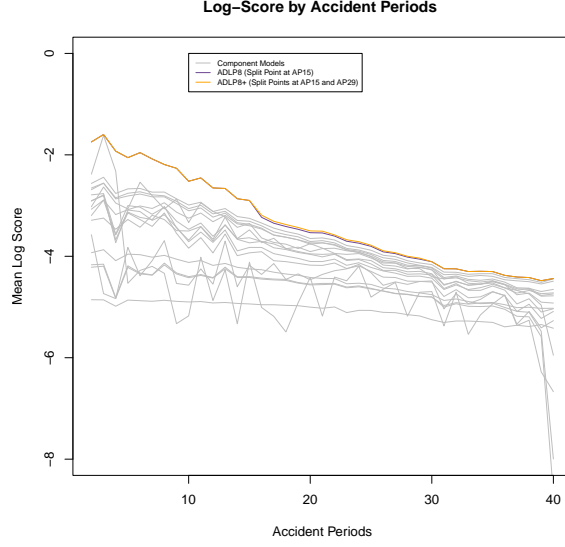


Figure B: Log Score Plot by Accident Periods: Comparison between $ADLP_8$ and $ADLP_8^+$

C.2. Combination Weights

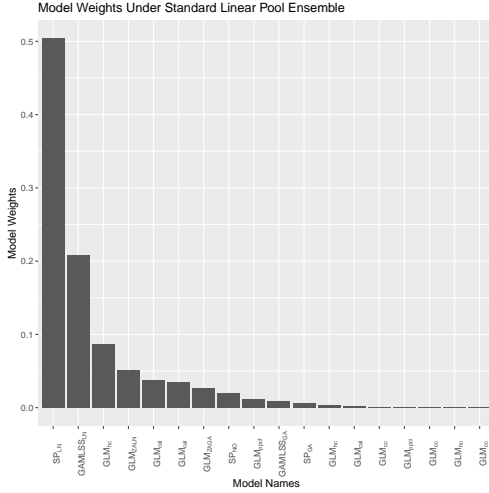


Figure C: Combination Weights under Stan-

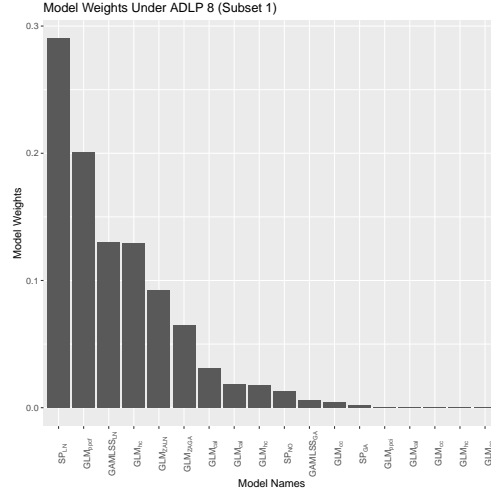


Figure D: Combination Weights in Subset 1 under $ADLP_8$

C.3. Why we should not use a single model aiming to capture all possible features: An illustrative example

In previous sections, we suggest the attempt to capture all possible features by using a single model is often not ideal. To provide a simple example to support our recommendation, two exploratory experiments are illustrated below. Firstly, we seek to build a model that combines the characteristics of both smoothing spline (i.e. SP_{LN}) and GAMLSS (i.e. $GAMLSS_{LN}$), which have the best and the second-best out-of-sample performance by Log Score; see Section 6.5. The newly developed model is constructed by adding a variance term (as a function of development periods) to SP_{LN} . By using (2.8) and (2.12), the mean and the variance structures of the new integrated model (denoted as $GAMLSS_{LN}^{SP}$) can be specified by (C.1) and (2.12).

$$\begin{aligned} E[Y_{ij}] &= g^{-1}(\eta_{1,i,j}) \\ &= \exp(s_{\theta_i}(i) + s_{\theta_j}(j)) \end{aligned} \quad (C.1)$$

$$\begin{aligned}\text{Var}[Y_{ij}] &= g^{-1}(\eta_{2,i,j}) \\ &= \exp(s_{\theta_j}(j))\end{aligned}\tag{C.2}$$

Table B compares the training Log Score (i.e. the mean Log Score in the in-sample data) and test Log Score (i.e. the mean Log Score in the out-of-sample data) attained by GAMLSS_{LN}^{SP} and SP_{LN} , respectively. As per Table B, although GAMLSS_{LN}^{SP} receives a higher training Log Score, its out-of-sample performance is inferior to SP_{LN} . Since the difference between SP_{LN} and GAMLSS_{LN}^{SP} is the additional dispersion term, the under-performance of GAMLSS_{LN}^{SP} relative to SP_{LN} might be explained by the fact that adding the additional dispersion term leads to over-fitting in this case.

Table B: Comparison of Training and Test Log Score: SP_{LN} and GAMLSS_{LN}^{SP}

Models	Training Log Score	Test Log Score
GAMLSS_{LN}^{SP}	-3.8633	-3.9836
SP_{LN}	-3.9427	-3.9658

In the second experiment, we combine SP_{LN} and GAMLSS_{LN} using the standard linear pooling strategy. The combination weights are therefore optimised using

$$\hat{\mathbf{w}} = \arg \max_w \frac{1}{|D^{val}|} \sum_{y_{ij} \in D^{val}} \ln(w \cdot \hat{f}_{SP}(y_{ij}) + (1-w) \cdot \hat{f}_{\text{GAMLSS}}(y_{ij})).\tag{C.3}$$

The weights allocated to SP_{LN} and GAMLSS_{LN} are 0.7304 and 0.2696, respectively. Based on Table C, the mean Log Score of the ensemble of GAMLSS and the smoothing spline, denoted as SLP_{GSP} , out-performs both SP_{LN} and GAMLSS_{LN}^{SP} .

The results from the first and the second experiment might be explained by the fact that GAMLSS_{LN}^{SP} , which is a combination of the GAMLSS and smoothing spline structure, does not explicitly specify the weight allocated to each structure, not to mention optimising the weights. Although modelling the dispersion term might lead to over-fitting, by applying a small weight to the GAMLSS model, the performance can still be improved. This phenomenon might be explained by the slight but not significant variation of dispersion across development periods; therefore, neither using a single model to model the the dispersion (e.g. GAMLSS_{LN}^{SP}) nor completely ignoring the dispersion (e.g. SP_{LN}) can optimally describe the data.

Consequently, an ideal solution is to consider both GAMLSS_{LN} and SP_{LN} , but apply a smaller weight to the former. This weights-allocation problem can then be easily solved by the linear pooling strategy.

Table C: Comparison of Log Score: SLP_{GSP} , SP_{LN} , GAMLSS_{LN}^{SP}

Models	Mean Log Score
SLP_{GSP}	-3.9467
SP_{LN}	-3.9670
GAMLSS_{LN}^{SP}	-3.9863